HHS Public Access

Author manuscript

J Physiol. Author manuscript; available in PMC 2022 August 01.

Published in final edited form as:

J Physiol. 2021 August ; 599(15): 3771–3797. doi:10.1113/JP281362.

Acute morphine blocks spinal respiratory motor plasticity via long- latency mechanisms that require toll-like receptor 4 signaling

Arash Tadjalli[1,2], **Yasin B. Seven**[1,2], **Abhisheak Sharma**[3], **Christopher R. McCurdy**[4], **Donald C. Bolser**[1,5], **Erica S. Levitt**[1,6], **Gordon S. Mitchell**[1,2]

[1]Breathing Research and Therapeutics Center, University of Florida, Gainesville, FL, 32610

[2]Department of Physical Therapy, University of Florida, Gainesville, FL, 32610

[3]Department of Pharmaceutics, University of Florida, Gainesville, FL, 32610

[4]Department of Medicinal Chemistry, University of Florida, Gainesville, FL, 32610

[5]Department of Physiological Sciences, University of Florida, Gainesville, FL, 32610

[6]Department of Pharmacology and Therapeutics, University of Florida, Gainesville, FL, 32610

Abstract

Opioid-induced respiratory dysfunction is a significant public health burden. While respiratory effects are mediated via mu opioid receptors, long-latency off-target opioid signaling through innate immune toll like receptor 4 (TLR4) may modulate essential elements of breathing control, particularly respiratory motor plasticity. Plasticity in respiratory motor circuits contributes to the preservation of breathing in the face of destabilizing influences. For example, respiratory long-term facilitation (LTF), a well-studied model of respiratory motor plasticity triggered by acute intermittent hypoxia, promotes breathing stability by increasing respiratory motor drive to breathing muscles. Some forms of respiratory LTF are exquisitely sensitive to inflammation and are abolished by even a mild inflammation triggered by TLR4 activation (e.g. via systemic lipopolysaccharides). Since opioids induce inflammation and TLR4 activation, we hypothesized that opioids would abolish LTF through a TLR4-dependent mechanism. In adult Sprague Dawley rats, pre-treatment with a single systemic injection of the prototypical opioid agonist, morphine, blocks LTF expression several hours later in the phrenic motor system—the motor pool driving diaphragm muscle contractions. Morphine blocked phrenic LTF via TLR4-dependent mechanisms because pre-treatment with (+)-naloxone—the opioid inactive stereoisomer and novel small molecule TLR4 inhibitor—prevented impairment of phrenic LTF in morphine-treated rats. Morphine triggered TLR4-dependent activation of microglial p38 MAPK within the phrenic motor

Corresponding author: Arash Tadjalli, PhD, Department of Physical Therapy, College of Public Health & Health Professions, University of Florida, 1225 Center Drive, PO Box 100154, Gainesville, FL, 32610, Phone: 352-273-6107, Fax: 352-273-6119, atadjalli@ufl.edu.

Author Contributions: AT, ESL, DCB and GSM: conception and design of research; AT and ESL: project administration and oversight; AT: performed neurophysiological experimental procedures/recordings, neurophysiology data analysis, tissue sample collection, immunohistochemistry and fluorescence microscopy imaging; YBS: performed image analysis, AS and CRM: performed quantification of blood serum morphine and metabolites; AT, ESL and GSM interpreted the data; AT: wrote the first draft of the manuscript; AT, ESL and GSM: manuscript revisions and final approval of manuscript.

Competing Interests: We confirm that we do not have any financial or non-financial competing interests to disclose.

system — a key enzyme that orchestrates inflammatory signaling and undermines phrenic LTF. Morphine-induced LTF loss may de-stabilize breathing, potentially contributing to respiratory side effects. We suggest minimizing TLR-4 signaling may improve breathing stability during opioid therapy by restoring endogenous mechanisms of plasticity within respiratory motor circuits.

Keywords

morphine; opioid; (+)-naloxone; toll-like receptor 4; phrenic motor neuron; spinal cord; neuroplasticity; intermittent hypoxia; inflammation; breathing

INTRODUCTION

Opioids are among the most frequently prescribed drugs worldwide, largely for the control of pain (Berterame *et al.*, 2016). Prototypical opioids, such as morphine, are the gold standard drugs of choice for pain management, although unfavorable side effects limit their use (Volkow & Collins, 2017). For example, decreased analgesic efficacy over time impedes treatment and is often associated with increased risk of abuse, motor and cognitive impairments, tolerance, and respiratory dysfunction (Gulur *et al.*, 2014; Dowell *et al.*, 2016). Among the undesirable side-effects, impaired breathing function, including respiratory failure, sleep-disordered breathing (e.g. sleep apnea) and airway muscle dysfunction are major contributors to morbidity and mortality from opioid use (Farney *et al.*, 2003; Christ *et al.*, 2006; Pattinson, 2008; Hajiha *et al.*, 2009; Savilampi *et al.*, 2013; Montandon & Horner, 2014; Savilampi *et al.*, 2014; Van Ryswyk & Antic, 2016).

Understanding mechanisms by which classical opioid signaling pathways depress breathing has been the focus of many studies (Pattinson, 2008; Boom *et al.*, 2012; Levitt *et al.*, 2015; Bachmutsky *et al.*, 2020; Palkovic *et al.*, 2020; Varga *et al.*, 2020). However, it is unknown if morphine, through an off-target signaling pathway, impacts essential elements in the control of breathing such as respiratory motor plasticity. Respiratory motor plasticity is an essential property of the respiratory control system, enabling respiratory circuits to adapt to recurring and/or prolonged changes in physiological or environmental conditions (Mitchell & Johnson, 2003; Devinney *et al.*, 2013; Gonzalez-Rothi *et al.*, 2015; Fuller & Mitchell, 2017). The main goal of this study was to determine whether a single acute systemic injection of morphine has long-lasting impact on the expression of plasticity in the phrenic motor system—the major motor pool driving inspiratory contractions of the diaphragm.

One well-studied model of respiratory motor plasticity is phrenic long-term facilitation (pLTF). pLTF is characterized by a long-lasting compensatory increase in phrenic motor output induced by brief exposures to intermittent, but not continuous hypoxia (Fuller *et al.*, 2000; Baker-Herman & Mitchell, 2002; McGuire *et al.*, 2003). Moderate acute intermittent hypoxia (mAIH) induces a form of pLTF that requires cervical spinal Gq-protein coupled serotonin type 2 activation (Tadjalli & Mitchell, 2019), reactive oxygen species (MacFarlane *et al.*, 2009), ERK 1/2 MAPK activity (Hoffman *et al.*, 2012), new BDNF protein synthesis and downstream TrkB signaling (Baker-Herman *et al.*, 2004; Dale *et al.*, 2017). This signaling cascade enhances respiratory drive transmission to phrenic motor neurons (Fuller *et al.*, 2003; Golder & Mitchell, 2005), increasing motor neuron activity and

diaphragm muscle contraction. pLTF may reflect a form of natural compensation, stabilizing breathing by increasing motor output, thereby offsetting/minimizing respiratory depression or recurrent apneas.

pLTF is highly sensitive to systemic inflammation; for example, acute inflammation induced by even a low dose of systemic lipopolysaccharide (LPS) blocks mAIH-induced pLTF (Vinit *et al.*, 2011; Huxtable *et al.*, 2013; Tadjalli *et al.*, 2021). LPS is a bacterial-associated endotoxin that signals through the pattern recognition the innate immune receptor, toll-like receptor 4 (TLR4). Immune signaling is a major contributor to the unwanted side effects of opioids, including tolerance and hyperalgesia (Raghavendra *et al.*, 2002; Cui *et al.*, 2008; Eidson & Murphy, 2013; Araldi *et al.*, 2019). Acute and chronic opioid use triggers pro-inflammatory responses by activation of TLR4 similar to endotoxins such as LPS (Christrup, 1997; Hutchinson *et al.*, 2008b; Hutchinson *et al.*, 2010; Lewis *et al.*, 2010; Wang *et al.*, 2012; Eidson *et al.*, 2017). This novel, off-target mechanism, does not require signaling through classical opioid receptors. Therefore, we reasoned that opioids may undermine mAIH-induced pLTF by activating TLR4.

Although downstream effectors of TLR4 signaling in the context of opioid use are not fully known, TLR4-mediated p38 mitogen-activated protein kinase (MAPK) activation initiates pro-inflammatory cascades, resulting in aberrant modulation of neural function (Hutchinson *et al.*, 2008a; Chen & Sommer, 2009; Hutchinson *et al.*, 2011; Winters *et al.*, 2017; de Freitas *et al.*, 2019; Deng *et al.*, 2019). P38 MAPK signaling is often associated with stimuli that are inflammatory or stressful and its activation is an important regulator of neural synaptic plasticity (Thomas & Huganir, 2004; Moult *et al.*, 2008; Collingridge *et al.*, 2010). Thus, in the context of this study, opioids may also activate p38 MAPK in spinal regions containing the phrenic motor nucleus. Since mAIH-induced pLTF is exquisitely sensitive to inflammation and morphine induces pro-inflammatory TLR4 signaling, we tested the hypotheses that: 1) acute systemic morphine delivery abolishes mAIH-induced pLTF; 2) acute morphine undermines pLTF by a TLR4-dependent mechanism; and 3) acute morphine induces TLR4-dependent upregulation of p38 MAPK phosphorylation/activity in the phrenic motor nucleus.

We demonstrate that acute systemic morphine delivery blocks mAIH-induced pLTF by mechanisms that persist even after serum morphine concentration dropped to levels not capable of inducing respiratory depression alone. Instead, we show that TLR4 activation is necessary for pLTF suppression by using a selective novel small molecule TLR4 inhibitor, (+)-naloxone, which is an opioid-inactive isomer (Iijima *et al.*, 1978; Labella *et al.*, 1979; Lewis *et al.*, 2012; Chin *et al.*, 2016; Wang *et al.*, 2016). Pre-treatment with TLR4 inhibitor attenuated the morphine-induced impairment of pLTF. Finally, using quantitative optical density immunofluorescence, we demonstrate that morphine increases microglial (but not neuronal) p38 MAPK phosphorylation in the phrenic motor nucleus, and that inhibition of TLR4 signaling prevents this effect, demonstrating that morphine enhances p38 MAPK activity via mechanisms that require TLR4 activation. Collectively, we show that impaired pLTF following morphine delivery is mediated via a long-latency, non-canonical signaling pathway independent of opioid receptor signaling. This finding is consistent with the idea that off-target opioid effects may remove an important endogenous stabilizing mechanism,

thereby contributing to respiratory depression and/or recurrent apneas. We suggest that TLR4 receptor inhibition may be a useful approach to separate beneficial (analgesia) versus unwanted opioid actions, improving opioid efficacy while preserving adequate breathing.

METHODS

Ethical Approval

Experiments were conducted on adult male Sprague Dawley rats (Charles River: Crl: CD-SD rats), weighing between 350 to 480 grams. Rats had access to food and water ad libitum and were kept in a 12-hour daily light-dark cycle. All procedures and experimental protocols were approved by the Institutional Animal Care and Use Committee at the University of Florida (Protocol # 201609515). Experiments performed in this manuscript also conform to the principles and regulations as described in the Editorial by Grundy (2015). All anesthetized animals were sacrificed via either transcranial perfusion, or anesthetic urethane overdose, permanently terminating heart rate, blood pressure and phrenic activity.

Drugs and Vehicles

Morphine sulfate and (+)-naloxone were obtained from the National Institute of Drug Abuse Drug Supply Program. Morphine and (+)-naloxone were dissolved in a sterile saline solution and protected from light exposure. Stock drug solutions remained viable at room temperature for up to 3 weeks, after which the drugs were discarded, and a fresh solution was made as needed. Drugs or vehicle (sterile saline) were administered *via* subcutaneous (s.c.) injections (lower left abdominal quadrant) 3 hours prior to beginning terminal experiments.

Morphine was delivered at a dose of 4 mg/kg (s.c.): a dose shown to activate inflammatory signaling that persists for hours (Hutchinson *et al.*, 2008a). This dose is predicted not to agonize mu opioid receptors effectively beyond 2 hours post-injection (Hutchinson *et al.*, 2008a), and is not expected to compromise overall activity such as locomotion or respiratory motor output. This was an important consideration in our studies since our goal was to experiment with long-latency morphine effects that could activate an inflammatory cascade without causing a persistent respiratory depression. (+)-Naloxone was administered at 10 mg/kg (s.c). (+)-Naloxone is an inactive enantiomer of the corresponding mu opioid receptor antagonist (Iijima *et al.*, 1978; Valentino *et al.*, 1983; Lewis *et al.*, 2012; Doyle & Murphy, 2018), and does not antagonize mu opioid receptors. Instead, (+)-naloxone antagonizes TLR4 (Hutchinson *et al.*, 2008b; Lewis *et al.*, 2012; Wang *et al.*, 2016). The (+)-naloxone dose of 10 mg/kg was chosen because it results in plasma concentrations in the pharmacologically active range (Hutchinson *et al.*, 2010; Lewis *et al.*, 2012), but without the off-target effects known to occur at higher doses (≥ 32 mg/kg) (Tanda *et al.*, 2016).

Surgical Procedures

Anesthesia was induced with 3% inspired isoflurane in a Plexiglas chamber, and maintained with a nose cone (60% O2 balance N2). After confirming absence of any foot-pinch withdrawal reflex, a midline ventral cervical incision was made in the neck, the trachea was exposed and sectioned below the larynx; a tracheal tube (polyethylene catheter; PE

240; Intramedic, MD, USA) was inserted into the trachea to deliver isoflurane and mixed gases via artificial ventilation (2.5% isoflurane in 60% O2/balance N2). Artificial ventilation was achieved with a rodent ventilator (Tidal volume = 0.7 ml / 100g body weight; Rodent Respirator model 683, Harvard Apparatus, South Natick, MA, USA; ventilator rate 70 breaths/min). A rapidly responding flow-through CO2 analyzer (Capnogard, Novametrix, Wallingford, CT, USA) was placed on the expired side of a Y-tube connected to the tracheal cannula to monitoring end-tidal PCO_2 ($PetCO_2$). The tail vein was cannulated (24 gauge, Surflo, Elkton, MD, USA) so that rats could be slowly converted from isoflurane to urethane anesthesia (2.1 mg/kg; i.v.). Conversion to urethane was carried out at least one hour before beginning experimental protocols. Absence of foot-pinch withdrawal reflexes was used to test adequacy of anesthesia; supplemental anesthetic was given as required. Once urethane conversion was complete, fluids were given through the same tail vein cannula to maintain acid-base balance (1.5–2.5 ml/hour, started ~1 hour after the beginning of surgery; 1:4 solution of 8.4% sodium bicarbonate mixed in standard lactated Ringer's solution). Body temperature was monitored with a rectal thermometer (Fischer Scientific, Pittsburgh, PA, USA) and maintained (37.5 ± 1°C) with a custom-made heated surgical table.

Rats were bilaterally vagotomized in the mid-cervical region to prevent entrainment of respiratory motor output with the ventilator, and paralyzed with pancuronium bromide (2 mg/kg; Sigma-Aldrich, St. Louis, MO, USA) to prevent the rats from "fighting" the ventilator. Flexible polyethylene tubing (PE 50; Intramedic MD, USA) was inserted into the femoral artery, and connected to a pressure transducer (Grass Instruments) to monitor arterial blood pressure. The same arterial line was also used to withdraw blood samples (70 ul) for blood gases measurements (i.e. PaO_2 and $PaCO_2$), acid-base balance and pH using a blood gas analyzer (ABL 90 Flex, Radiometer, Copenhagen, Denmark). Using a dorsal approach, the left phrenic nerve was isolated, cut distally and de-sheathed. Nerves were kept moist by a saline-soaked cotton ball until ready to be placed in suction recording electrodes to record nerve activity.

Electrophysiological Recordings

Custom-made glass suction electrodes were filled with 0.9% saline. Nerve activity was amplified (10K, A-M systems, Everett, WA), filtered (bandpass 100–5000 Hz), integrated (time constant 50 msec), digitized (Micro1401, Cambridge Electronic Design, UK) and analyzed using Spike 2 software (Cambridge Electronic Design, UK; version 8.08). Since peak amplitude of integrated inspiratory phrenic nerve bursts correlates with tidal volume in spontaneously breathing animals (Eldridge, 1976), integrated phrenic nerve burst amplitude served as an index of respiratory motor output. Inspiratory phrenic burst amplitude was determined immediately prior to blood samples drawn during baseline & hypoxic conditions, and at 30 and 60-minutes post-AIH. Measurements were made at equivalent times in time control experiments that did not receive AIH.

Immunohistochemical Experiments

Triple immunofluorescence labeling was employed to stain for phospho-p38 MAPK, CD11b (microglial marker) and NeuN (neuronal marker). Rats used for immunohistochemistry did not undergo neurophysiological procedures. Approximately 4.5 hours following injections of

the vehicle or drugs (see Study 3 below), rats were briefly anesthetized with isoflurane (~4-min under 3.5% isoflurane) and immediately perfused transcardially with ice-cold phosphate buffered saline (PBS, pH 7.4) followed by 4% buffered paraformaldehyde (PFA, pH 7.4). Cervical segment of the spinal cord (C3-C5) was excised, post-fixed in 4% paraformaldehyde overnight, and cryoprotected in 30% sucrose at 4°C. 40μm transverse sections were cut using a freezing microtome (Leica SM 2010R, Germany) and stored in anti-freeze solution (−20°C) until the day of staining. Transverse tissue sections were numbered sequentially and 2 sections per spinal segment (C3, C4 and C5) were used to represent C3-C5 for each animal (total of 6 spinal sections per animal). Free-floating sections were washed in 0.1M PBS containing 0.1% Triton-X100 (PBS-TX; 3 × 5-minute washes). Tissues were then blocked with 5% normal donkey serum (GeneTex, CTX30972) for 1 hour at room temperature to block non-specific binding sites. Staining was performed by incubating free-floating tissues with primary antibodies against CD11b (mouse host, 1:1000, EMD Millipore, USA), phospho-p38 MAPK (rabbit host, 1:500, Cell Signaling Technology, Inc.) and NeuN (chicken host; 1:1500, EMD Millipore, USA) over night at 4C (diluted in 2.5% donkey serum in PBS). Tissues were then washed, followed by incubation with secondary antibodies (1 hour room temperature in PBS-0.1% TX) to label CD11b (Donkey anti-mouse Alexa Fluor 488, 1:1000, Invitrogen), phospho-p38 MAPK (Donkey anti- rabbit, 1:500, Alexa Fluor 555, Invitrogen, USA), and NeuN (Donkey anti-chicken Alexa Fluor 647, 1:1500, Jackson Immuno Research, USA). Sections were then immediately washed in PBS and mounted on slides using VectaShield antifade hard-set mounting medium (Vector Laboratories, California, USA, Product # H-1400).

Analysis of serum morphine and metabolites

Serum was collected from a group of rats approximately 4.5 hours following a single systemic injection of morphine (s.c., 4mg/kg; n=6). Whole blood was collected into an anti-coagulant free serum separation plastic tube (600 ul per animal; BD Microtainer SST Gold Top, Item Number BD365967; Becton, Dickinson and Company, NJ, USA). Blood was allowed to clot at room temperature for 30-minutes. Clotted samples were then centrifuged at 2500 ×g for 10 minutes at 4 °C. Serum was removed and stored in cryovials at −80 °C until ready for analysis.

Materials and reagents for serum analysis—Commercially available standards (purity >98%) for morphine, morphine-3-glucuronide, morphine-6-glucuronide, morphine-D3, morphine-3-glucuronide-D3, and morphine-6-glucuronide-D3 were purchased from Cerilliant (Round Rock, TX, USA). LC-MS grade water, acetonitrile, and formic acid were obtained from Fisher Scientific (Fair Lawn, NJ, USA).

Analysis of serum morphine, morphine-3-glucuronide, and morphine-6-glucuronide—A bioanalytical method for the simultaneous quantification of morphine, morphine-3-glucuronide, and morphine-6-glucuronide was developed using an Acquity I-Class Plus UPLC coupled with Waters Xevo TQ-S Micro triple quadrupole mass spectrometer (Milford, MA, USA). An isocratic method using a mobile phase consisting of water containing 0.1% formic acid and acetonitrile on a Waters Acquity CSH C18 column (1.7 μm, 2.1 × 100 mm) was used, and a base-to-base peak separation was achieved for the

analytes sharing the mass transitions, 3- and 6-glucuronide of morphine. The composition of water containing 0.1% formic acid and acetonitrile was 95 and 5%, respectively, and the flow rate of the mobile phase was 0.3 ml/min. Ionization of morphine, morphine-3-glucuronide, and morphine-6-glucuronide was achieved using electrospray ionization (ESI) in positive mode. Morphine-D3, morphine-3-glucuronide-D3, and morphine-6-glucuronide-D3 were used as internal standards for morphine, morphine-3-glucuronide, and morphine-6-glucuronide, respectively. The mass spectral analysis was achieved by multiple reaction monitoring (MRM), and compound parameters for analytes and internal standards are mentioned in Table 1.

A protein precipitation method using acetonitrile containing 0.1% v/v formic acid and internal standards (10 ng/ml, each) (100 μl) was used for the cleanup of serum samples (25 μl). Test samples were analyzed along with the freshly prepared calibration (1, 2.5, 5, 25, 50, 100, 150, and 200 ng/ml) and quality control standards (1, 3, 90, and 180 ng/ml) in drug-free serum samples. The method was linear for a calibration range of 1–200 ng/ml for morphine and its 3- and 6-glucuronide metabolites. Accuracy and precision for the method were within the specified limit, and dilution integrity (5X) was performed to analyze the test samples above the linearity range.

Experimental Protocols

At least 1 h after conversion to urethane anesthesia, apneic and recruitment CO_2 thresholds of respiratory nerve activity was determined by lowering inspired CO_2 (or increasing ventilation rate in some cases) levels until rhythmic respiratory nerve activity ceased. After ~60 seconds, inspired CO_2 was slowly increased until rhythmic respiratory nerve bursts resumed. The end-tidal PCO_2 at which respiratory nerve activity stopped and then resumed were considered the apneic and recruitment thresholds, respectively. Baseline conditions were then established by holding end-tidal PCO_2 ~2 mmHg above the recruitment threshold and allowing sufficient time to establish stable nerve activity (> 20min). During baseline recordings, an arterial blood sample was taken to document baseline blood gas levels. Arterial PCO_2 was maintained isocapnic (± 2 mmHg) with respect to this baseline value throughout experiments by actively manipulating inspired carbon dioxide concentration and/or ventilation rate. Baseline oxygen levels (~60% inspired oxygen, balance N_2 and CO_2; $PaO_2 \geq 150$ mmHg) were maintained for the duration of experiments except during hypoxic challenges; targeted arterial PaO_2 levels during hypoxic episodes were 35–50 mmHg. At the end of every experimental recording period, we assessed phrenic motor output response to a chemosensory stimulus composed of combined hypoxia and hypercapnia. Chemoreflex activation of breathing is an important component of the ventilatory control system. For example, chemosensory responses to hypoxia and hypercapnia are important feedback mechanisms that are critical for maintenance of blood gas homeostasis, as well as eliciting appropriate reflex ventilatory responses when facing challenges that compromise adequate lung ventilation. Chemosensory stimulation at the end of each neurophysiological experiment consisted of an inspired gas mixture consisting of 10% O_2, 7% CO_2 and balance N_2 (total duration of two minutes).

Study 1 – Does acute systemic morphine block phrenic long-term facilitation?—Before determining if acute systemic morphine administration affects AIH-induced pLTF expression, we ensured that pLTF was present in sham control rats pre-treated with systemic vehicle (i.e. saline). In a group of rats that were injected with saline (1 ml/Kg; n=6), surgical procedures began 3 hours later following the initial injection. By the time rats had undergone full surgical procedures and baseline nerve recordings were established, 4.5 hours had lapsed since the initial systemic vehicle injection. At this time point (~ 4.5 hours post-injection) the pLTF protocol was executed. To trigger pLTF, rats were exposed to 3, 5-min episodes of isocapnic hypoxia (~12% inspired O2; CO2 kept ± 2 mmHg from baseline) separated by 5-min intervals of baseline O2 conditions. After the third hypoxic episode, rats were returned to baseline inspired O2 levels and biological variables were recorded for another 60-minutes.

To determine if systemic morphine blocks pLTF, a separate rat group was injected with morphine (4 mg/kg, subcutaneous; n=8), and surgical procedures commenced 3 hours following the injection as described. During acute neurophysiological recordings, rats were exposed to the same pLTF AIH protocol described above (~4.5 hours post-morphine injection). An additional group of time-matched, morphine-injected rats without AIH exposures were used to assess the stability of respiratory motor output during the neurophysiological recording period (i.e. time control for morphine treatment; n=6).

Study 2 – Does systemic (+)-naloxone pretreatment preserve phrenic LTF after morphine delivery?—In study 1, we determined that systemic morphine blocks pLTF expression. Thus, we aimed to determine whether morphine blocked pLTF via TLR4-dependent mechanisms. Rats (n=6) were injected with (+)-naloxone (TLR4 antagonist; 10mg/kg; s.c.), and 20-minutes later, they were injected with morphine (s.c.). 3 hours post-morphine injection, rats were anesthetized, and underwent the same surgical procedures as described. Approximately 4.5 hours following the initial injection, pLTF was assessed as described above. We hypothesized that pre-treatment with (+)-naloxone would prevent the morphine-induced impairment of pLTF. An additional rat group received (+)-naloxone followed by systemic morphine without AIH exposure; this group served as time control for combined (+)-naloxone and morphine treatment (n=6).

Study 3 – Does morphine increase p38 MAPK phosphorylation levels in the ventral horn of the cervical spinal cord?—Since p38 MAPK has been implicated in opioid-induced inflammatory signaling, we evaluated morphine effects on p38 MAPK phosphorylation levels in the medio-lateral C3-C5 ventral horn of the cervical spinal cord — a neuroanatomical area containing the phrenic motor nucleus. Transverse slices of cervical spinal tissue sections were harvested from sham vehicle treated (n=3) rats ~4.5 hours following vehicle injections (s.c.), the time point at which the AIH pLTF protocol would have been implemented in neurophysiology rat groups. Spinal tissues were also collected at an equivalent time from separate rats receiving either morphine (n=4), or combined (+)-naloxone and morphine (n=3). Triple immunofluorescence labeling was used to stain for phospho-p38 MAPK, CD11b (microglial marker) and NeuN (neuronal marker). Quantitative

image analysis was performed to quantify differences in phosphorylated p38 MAPK levels in neurons and microglia within each experimental group.

Images were captured using a high-resolution microscope designed for multichannel fluorescence microscopy (Keyence-972032 BZ-X710, Keyence Co., Osaka, Japan). All images used for analysis were captured at 20× magnification. CD11b immune-labelling was detected using a GFP filter (BZ-X, model no: OP-87763) at an excitation filter of 472/30 nm. Phospho-p38 MAPK labelling was detected using a TexasRed filter (BZ-X, model no: OP-87765) at an excitation filter range of 555/40 nm. NeuN labelling was detected using a Cyanine-5 filter (BZ-X, model no: OP-87766) at an excitation range of 647/40 nm. Exposure times of 1/15 seconds for phospho-p38 MAPK, 1/5 seconds for CD11b, and 1/10 seconds for NeuN were used for imaging immunofluorescence in the spinal region of interest. In combination, 94 spinal cord sections were imaged in this study. Within each spinal section, three fluorescent markers were captured: images for CD11b, NeuN and phospho-p38 MAPK, for a total of 276 individual images all combined. 105 (34 spinal cord sections) total images were analyzed for morphine treated rats, 78 (28 spinal cord sections) images were analyzed for (+)-naloxone and morphine treated rats and 93 (32 spinal cord sections) images were analyzed for vehicle treated rats.

DATA ANALYSIS

Respiratory nerve activities were analyzed using Spike 2 software (Cambridge Electronic Design, UK; version 8.08). Integrated phrenic nerve inspiratory burst amplitudes were averaged over 1-minute bins at each experimental time point. Activities were analyzed during baseline, hypoxia, and at 30 and 60-minutes post-hypoxia. Changes (Δ) in nerve burst amplitudes were normalized and reported as percentage change from baseline (baseline = 0). Therefore, any value below zero is a decrease whereas values above zero are increases relative to baseline. Burst frequencies were also presented as number of breaths per minute. Respiratory activities were also analyzed at equivalent time points in time matched control animals that were not exposed to hypoxia. We also measured and analyzed mean arterial pressure (MAP), arterial CO2 pressure (PaCO2), arterial O2 pressure (PaO2), pH and standard base excess (SBEc) (Table 2). Values for these biological variables were not normalized and were presented as absolute values in respective figures and tables. Phrenic nerve inspiratory amplitude was also quantified during a chemosensory challenge at the end of each recording period. This was accomplished by analyzing steady-state maximal phrenic nerve amplitude for one minute during hypoxic hypercapnia (10% inspired O2 combined with 7% inspired CO2). Statistical comparisons between treatment groups were made using a One-Way ANOVA followed by the Tukey significance post hoc test for individual comparisons (SigmaPlot version 14; Systat Software Inc., San Jose, California, USA). Baseline phrenic nerve amplitudes, baseline respiratory frequency, baseline blood pressure, acute short-term hypoxic phrenic responses, and blood pressure change during hypoxia were also compared using a one-way ANOVA with Tukey post hoc test. Differences between groups were considered significant if $p < 0.05$. All average group data are presented with standard deviation.

Immunofluorescence images were analyzed using a custom-written MATLAB algorithm (MathWorks, Natick, MA, USA) designed for quantification of fluorescence intensities for molecules of interest in the ventral horn of the cervical spinal cord (a well-defined anatomical region containing phrenic motor neurons). The analysis was conducted by an investigator who was blinded to the experimental conditions. The algorithm identified CD11b and NeuN-labelled cells, and quantified signal intensity of phospho-p38MAPK immune-reactivity in each cell type. Methods for protein-specific signal intensity quantification within the ventral horn of the cervical spinal cord have been previously described elsewhere (Seven *et al.*, 2018) in detail. CD11b (green color) and NeuN positive (purple color) cells were located within the ventral horn of the cervical spinal cord (cervical segments C3-C5) using a custom adaptive thresholding algorithm in MATLAB. The adaptive threshold was calculated by constructing a pixel intensity histogram from the image. First, a pixel intensity histogram is constructed in the immediate region of each detected cell in the ventral horn. The pixel intensity corresponding to fixed percentile value was used as the threshold value across all images to identify each cell type of interest. The pixels above the adaptive threshold were considered CD11b and NeuN-positive. Selection of a fixed percentile threshold returns a higher threshold value for an image with high signal and background intensities and a lower threshold value for an image with low signal and background intensities. CD11b and NeuN-positive images were binarized using the adaptive threshold, thus, CD11b and NeuN-positive areas were assigned the value of unity, whereas CD11b and NeuN-negative areas were set to zero. Intensity of the p38 MAPK labelling (red color) was calculated by averaging the pixel intensities within each identified cell type. The coordinates of CD11b and NeuN-positive pixels/areas were used to measure fluorescence intensities of phospho-p38 MAPK. Within each cell type, minimal detectable staining for “p38 MAPK” is expected due to minimal cellular auto-fluorescence that occurs with most staining procedures. Minimal detectable staining is a qualitative feature indicating the difference between the signal and the background fluorescence intensities. Although, we subtract general diffuse background fluorescence in our analyses, non-specific binding fluorescence and cellular auto-fluorescence remain throughout the cell bodies and projections. On the other hand, phospho-p38 MAPK positive regions are localized at the nucleus and clearly brighter than the background staining in other compartments of the cell. Therefore, final fluorescence intensities were determined after subtraction of local background labeling by determining the median value. For statistics, analyses of multiple comparisons were performed by ANOVA with Tukey’s significant difference test as post hoc test.

RESULTS

Baseline physiologic measurements.

To determine if morphine had long-latency effects on respiratory motor plasticity, rats were pretreated with vehicle or morphine (4 mg/kg) 3 hours prior to initiation of LTF experiments. A second group of rats were pretreated with the TLR4 inhibitor, (+)-naloxone (10 mg/kg), 20-minutes prior to morphine. Baseline phrenic nerve burst amplitude was compared among all groups, including time controls and mAIH exposed rats. There was no significant difference in baseline phrenic nerve amplitudes in any group (p =

0.185 in the overall ANOVA, Fig. 1A). This demonstrated that 1) none of the drug injections affected basal phrenic nerve motor output during neurophysiological recordings, and 2) normalization to baseline measurements as a percentage change from baseline was appropriate to quantify and compare the magnitude of phrenic nerve amplitude in various treatment groups (see sections above). Like baseline nerve burst amplitude, there was no difference in baseline breathing frequency comparing the various treatment groups ($p = 0.843$ in the overall ANOVA; Fig. 1B). This suggested that in the time frame of our neurophysiological recordings, which was 4.5 hours following morphine or vehicle administration, drug treatments did not elicit a detectable depression of breathing as far as breathing frequency or motor drive (i.e. burst amplitude) were concerned.

We also compared the short-term hypoxic phrenic response in groups that were exposed to moderate AIH (Fig. 2A and B). As expected, isocapnic hypoxic episodes triggered a robust increase in phrenic nerve burst amplitude, however, this increase was similar among treatment groups (vehicle: 61 ± 26%; morphine: 53 ± 24%; TLR4-inhibitor + morphine: 71 ± 24% increase above baseline; $p < 0.001$ versus baseline in each group; $p = 0.270$ for the difference among groups as determined by the ANOVA). Similarly, we found no difference in the short-term hypoxic frequency response comparing the groups that were exposed to mAIH ($p = 0.892$ in the overall NOVA). Thus, drug treatments did not have long-lasting effects on the short phrenic responses during acute intermittent hypoxic exposures.

We next compared mean arterial blood pressure (MAP) during baseline conditions, as well as during hypoxic episodes (Fig. 2A and C). No difference in baseline MAP were detected (vehicle: 99 ± 11 mmHg; morphine: 109 ± 13 mmHg; TLR4-inhibitor + morphine: 103 ± 11 mmHg; $p = 0.225$). As expected, there was a significant decrease in mean arterial pressure during hypoxic episodes in each group ($p < 0.001$, within each group), but MAP during hypoxia did not differ between groups (vehicle: 54 ± 21 mmHg; morphine: 53 ± 11 mmHg; TLR4-inhibitor + morphine: 56 ± 13 mmHg; $p = 0.927$ between groups).

Circulating levels of morphine and its metabolites

The lack of significant differences in baseline physiologic variables (breathing frequency, phrenic amplitude and MAP) between morphine and vehicle-pretreated rats suggests that the pretreatment time was sufficient for morphine to be metabolized and no longer circulating in physiologically relevant quantities at the start of our neurophysiological recordings. To confirm this, in a separate rat group (n=6), we measured serum levels of morphine and its two primary metabolites: morphine-3-glucuronide (M3G) and morphine-6-glucuronide (M6G). Serum was collected ~4.5 hours after a single acute morphine injection — an equivalent time delay to the execution of pLTF protocol in neurophysiological recordings. Morphine serum concentration was 15.5 ± 6 ng/ml, M3G was 323.7 ± 147 ng/ml and M6G was below the lower limit of quantification (<1 ng/ml) (Table 3). Lack of serum M6G was consistent with previous published findings, indicating that morphine is not metabolized to M6G in rats (Kuo *et al.*, 1991). Representative detection traces by mass spectral analysis as achieved by multiple reaction monitoring is shown in Figure 3.

Morphine blocks mAIH-induced phrenic long-term facilitation

To determine if acute morphine delivery affects mAIH-induced pLTF, rats were pre-treated with morphine (4 mg/kg, s.c.) 3 hours prior to initiation of experiments. Results were compared to vehicle-treated controls. Representative traces of integrated phrenic activity before, during and after mAIH are shown in Figure 4. Vehicle-treated control rats displayed a persistent increase in phrenic amplitude following mAIH, consistent with many previous published reports from our laboratory (Baker-Herman *et al.*, 2004; Devinney *et al.*, 2015; Tadjalli & Mitchell, 2019). 60-minutes post-mAIH phrenic nerve burst amplitude was significantly increased by 55 ± 11% above baseline levels, confirming the presence of pLTF (Fig. 4i and Fig. 5; n=6; $p < 0.0001$). In contrast, pretreatment with systemic morphine abolished mAIH-induced pLTF (8 ± 24% increase above baseline 60-min post-AIH; $p = 0.226$; Fig. 4ii and Fig. 5; n=8); phrenic nerve burst amplitude remained close to baseline levels throughout the post-hypoxic period. Morphine alone had no lasting effect on the stability of phrenic motor output in the time frame of these studies since phrenic output remained unchanged relative to baseline in time control rats (4 ± 20% above baseline at 60-min; $p = 0.916$; Fig. 4iv and Fig. 5; n=6). At 60-minutes post-mAIH phrenic burst amplitude was significantly greater in vehicle-treated rats exposed to mAIH versus morphine + mAIH ($p= 0.0028$) or morphine treatment alone ($p = 0.0003$). Thus, morphine pre-treatment activates mechanisms that block mAIH-induced pLTF.

Systemic morphine blocks phrenic long-term facilitation via mechanisms that require TLR4 signaling

Even a mild systemic inflammation triggered by lipopolysaccharides (LPS)—endotoxins that signal through TLR4 — undermines pLTF expression (Vinit *et al.*, 2011; Huxtable *et al.*, 2013). Since morphine is known to activate inflammatory cascades via TLR4 signaling, and systemic morphine pre-treatment blocks pLTF expression (Figure 4 and 5), we reasoned that morphine may block pLTF in a manner parallel to LPS endotoxins. Thus, we hypothesized that blocking TLR4 signaling prior to morphine delivery will prevent the impairment of pLTF. To block TLR4 signaling we used (+)-naloxone, which is the opioid inactive stereoisomer of the prototypical opioid antagonist naloxone. Unlike (−)-naloxone, which has an affinity for mu opioid receptors of 1 nM, (+)-naloxone has an affinity of greater than 10,000 nM for mu opioid receptors and is considered opioid receptor inactive (Iijima *et al.*, 1978; Valentino *et al.*, 1983). Rather, (+)-naloxone blocks TLR4 receptor signaling in vitro and in vivo (Hutchinson *et al.*, 2008b; Hutchinson *et al.*, 2010; Wang *et al.*, 2016). Two groups received the TLR4 inhibitor: one group received the TLR4-inhibitor followed by morphine without mAIH (time control) and another group received the same drug treatment followed by exposures to mAIH.

Pretreatment with the TLR4 inhibitor, (+)-naloxone, prevented the morphine-induced impairment of pLTF; at 60-minutes post-mAIH, phrenic burst amplitude was significantly increased by 50 ± 6% above baseline levels ($p < 0.0001$; Fig. 4iii and Fig. 5; n=6). The magnitude of pLTF in rats that received the combination of TLR4 inhibitor and morphine was not different compared to vehicle-treated controls (vehicle + mAIH), demonstrating that the TLR4 inhibitor fully prevented the morphine-induced impairment of pLTF (50 ± 6% versus 55 ± 11% above baseline; $p = 0.655$). In time-control rats injected with the TLR4

inhibitor and morphine (without mAIH; n=6), there was no discernable effect on phrenic motor output since phrenic burst amplitude did not change compared to baseline throughout the 60-minute recording period (5 ± 16% above baseline at minute 60; p = 0.747; Fig. 4v and Fig. 5).

(+)-Naloxone does not interfere with respiratory depressive actions of morphine

Since (+)-naloxone prevented morphine-induced pLTF impairment, we hypothesized that morphine blocked phrenic motor plasticity via TLR4 signaling. The next aim was to ensure that (+)-naloxone did not antagonize mu opioid receptors. Thus, in separate rat groups, morphine (4 mg/kg, sc) was administered while monitoring phrenic nerve activity. In these anesthetized rats, morphine caused potent depression, silencing phrenic nerve activity (Fig. 6A). We then questioned if acute morphine-induced respiratory depression could be reversed using (+)-naloxone, which would indicate mu opioid receptor antagonism. However, (+)-naloxone (10 mg/kg, sc) administration had no effect on acute morphine-induced respiratory depression since phrenic nerve activity remained absent (Fig. 6A and B). We then administered racemic (+/−)-naloxone, which contains the opioid active stereoisomer (−)-naloxone. In contrast to (+)-naloxone, racemic naloxone (1 mg/kg, sc), quickly reversed respiratory depression, fully restoring phrenic motor output (Fig. 6B; 61 ± 16 % increase above baseline after racemic naloxone injection; p = 0.0005). To control for the time difference between morphine administration and injection of antagonist, in a separate group of rats, we also administered (+)-naloxone at the same time as racemic naloxone in the previous experiments. (+)-Naloxone again had no effect on morphine-induced respiratory depression (Fig. 6C) since phrenic nerve activity remained absent. These findings demonstrate that, at the concentrations employed in this study, (+)-naloxone does not antagonize mu opioid receptors, consistent with previous literature reports (Iijima *et al.*, 1978; Valentino *et al.*, 1983).

Morphine alters maximal chemoreflex activation of phrenic motor output

Chemoreflex responses to hypoxia and hypercapnia are critical for maintenance of adequate breathing and for appropriate ventilatory responses in conditions that hinder lung ventilation, such as opioid-induced respiratory depression (Pattinson, 2008). Therefore, we determined if morphine affects phrenic responses to maximal chemoreflex activation during hypoxic hypercapnia (Fig. 7 and 8). In vehicle-treated rats exposed to mAIH, hypoxic hypercapnia triggered a 141 ± 30% increase in inspiratory phrenic nerve burst amplitude ($p < 0.0001$). This increase was greater compared to rats that received morphine + mAIH (83 ± 33% baseline; p = 0.034 comparing the means), or morphine alone (68 ± 25% baseline; p = 0.006 comparing the means). There was a trend for the TLR4 inhibitor, (+)-naloxone, to attenuate the morphine-induced inhibition of maximal chemoreflex responses. In mAIH-exposed rats that received the TLR4 inhibitor prior to morphine, hypoxic hypercapnia triggered a 133 ± 29% increase in phrenic amplitude ($p < 0.0001$), a response significantly larger than in morphine time controls or in rats that received morphine + mAIH (p = 0.003 in the overall ANOVA). Further, maximal chemoreflex responses were not different versus rats receiving vehicle + mAIH, demonstrating full chemoreflex restoration (p = 0.679 comparing vehicle + mAIH versus TLR4-inhibitor + morphine + mAIH). Thus, morphine-induced blunting of maximal chemoreflex responses may involve mechanisms that require TLR4 signaling.

However, there were no significant differences in chemoreflex responses when comparing TLR4-inhibitor + morphine time controls, morphine time controls, or morphine + mAIH (morphine time controls: 68 ± 25%; morphine + mAIH: 83 ± 33% baseline; TLR4-inhibitor + morphine time controls: 100 ± 53 %, p = 0.374).

Morphine enhances cervical spinal microglial p38 MAPK phosphorylation via mechanisms that require TLR4 signaling

Our next aim was to determine whether morphine-induced deficits in pLTF are paralleled by p38 MAPK activation— a well characterized MAPK pathway downstream from TLR4 known to orchestrate inflammatory cascades. To determine whether morphine modulates p38 MAPK phosphorylation levels, we evaluated morphine effects on dually phosphorylated (enzymatically activated) p38 MAPK expression in the ventral horn of the C3-C5 segment of the cervical spinal cord (an anatomical region containing the phrenic motor nucleus) using optical density immunofluorescence. We evaluated p38 MAPK phosphorylation levels in both CD11b and NeuN-positive cells—markers for microglia and neurons, respectively (Fig. 9). Results were compared to vehicle control rats and a separate rat group that received the TLR4 inhibitor before morphine injections. In vehicle control rats, ventral spinal CD11b and NeuN-positive cells displayed minimal detectable phospho-p38 MAPK staining (Fig. 9; n=3 rats; 93 images in total). After acute morphine delivery (~4.5 hours post-drug injection; n=4 rats; 105 images in total), phospho-p38 MAPK was significantly increased in CD11-b positive cells (23 ± 7% increase in phospho-p38 MAPK intensity in morphine-treated versus vehicle-treated controls, Fig. 9 Niii; p=0.025). While morphine increased p38 MAPK phosphorylation in CD11b-positive microglia, no significant change was observed in NeuN-positive cells (1 ± 6% change in phospho-p38 MAPK staining intensity in morphine treated rats versus vehicle controls; p=0.20). Thus, morphine enhanced p38 MAPK phosphorylation/activation in ventral cervical spinal microglia, but not neurons.

Next, we analyzed p38 MAPK optical density in rats pre-treated with the TLR4 inhibitor before morphine delivery. In rats that were pretreated with the TLR4 inhibitor (n=3 rats; 78 images in total), morphine no longer increased microglial p38 MAPK phosphorylation (7 ± 9 % decrease in microglial p38 MAPK staining intensity versus vehicle controls; p = 0.191; Fig. 9 Niii). This was in sharp contrast to rats treated with morphine alone since we had observed a significant increase in p 38 MAPK phosphorylation with morphine treatment alone (see above). Thus, in the time frame of our studies, morphine enhances microglial p38 MAPK activity by a mechanism that requires TLR4 signaling. Rats receiving the TLR4 inhibitor followed by morphine did not exhibit significant change in neuronal p38 MAPK signaling (2 ± 5 % increase in neuronal p38 MAPK intensity versus vehicle controls; p = 0.154; Fig. 9 Niii).

DISCUSSION

This study revealed novel findings concerning the effect of acute morphine delivery on the expression of mammalian spinal respiratory motor plasticity. We showed that phrenic LTF, a form of hypoxia-induced spinal respiratory motor plasticity, is abolished by a single systemic injection of morphine given several hours earlier. The effect of morphine on

phrenic LTF was due to long-latency mechanisms because phrenic LTF was blocked even after circulating morphine levels fell below values normally required for mu-opioid receptor-induced respiratory depression. Instead, morphine-induced deficits in pLTF expression involved components of the innate immune signaling, since systemic inhibition of TLR4 receptors — pattern recognition innate immune receptors — prevented morphine-induced deficit in pLTF expression. In addition, a single morphine injection activates p38 MAPK within cervical spinal microglia, an effect blocked by systemic TLR4 inhibition. Since p38 MAPK—an important regulator of inflammatory signaling and pLTF— is activated by opioid-induced TLR4 signaling, TLR4 signaling via p38 MAPK may play a key role in linking the innate immune response and plasticity inhibiting mechanisms in the phrenic motor system. Our results suggest that TLR4 signaling is a key link between the innate immune response and plasticity promoting mechanisms within spinal respiratory motor circuits following acute morphine delivery. These results have important implications concerning the off-target, long-latency impact of even a single opioid dose on the induction of compensatory mechanisms, such as pLTF, and suggest a novel mechanism of opioid-induced respiratory instability.

The opioid inactive stereoisomer of naloxone, (+)-naloxone, was used to block TLR4 receptors (Watkins *et al.*, 2009). Naloxone, which is a prototypical opioid receptor antagonist, has two isoforms. (−)-Naloxone is a competitive antagonist at mu opioid receptors with an affinity of 1 nM. In contrast, (+)-naloxone has an affinity for mu opioid receptors greater than 10,000 nM, and is therefore considered opioid inactive (Iijima *et al.*, 1978; Valentino *et al.*, 1983). Consistent with this, (+)-naloxone does not bind directly to TLR4. Rather, (+)-naloxone inhibits TLR4 signaling by binding to myeloid differentiation protein 2 (MD-2), the co-receptor for TLR4 (Hutchinson *et al.*, 2010). In silico docking studies have shown that (+)-naloxone and morphine bind in the LPS binding pocket of MD-2, and deletion of TLR4 eliminates analgesia potentiating effects of (+)-naloxone (Hutchinson *et al.*, 2010; Wang *et al.*, 2012). The doses of (+)-naloxone used in vivo have varied significantly (4 – 100 mg/kg). We chose a dose on the lower end (10 mg/kg) because doses greater than 32 mg/kg may be non-specific (Tanda *et al.*, 2016). A similar dose of (+)-naloxone did not have effects on the morphine metabolite morphine-6-gluronide to induce analgesia, suggesting that (+)-naloxone does not interfere with mu opioid receptor signaling (Doyle & Murphy, 2018). In addition, we confirmed that (+)-naloxone does not interfere with morphine-induced respiratory depression, similar to previous findings with fentanyl-induced respiratory depression (Zwicker *et al.*, 2014). Thus, the actions of (+)-naloxone, particularly at the dose we used, are most likely due to actions on TLR4, and not opioid receptors. As previously demonstrated, TLR4 activation by LPS does indeed block pLTF expression (Tadjalli *et al.*, 2021). Because (+)-naloxone is a potent and selective blocker of TLR4 signaling, we suggest that presence of pLTF in morphine-treated rats that received (+)-naloxone was due to inhibition of TLR4 signaling.

Acute opioid effect on neuro-adaptive behaviors

Long-term opioid use leads to unfavorable side effects such as tolerance, dependence, and hyperalgesia (Cui *et al.*, 2006; Cui *et al.*, 2008; Watkins *et al.*, 2009; de Freitas *et al.*, 2019). The underpinnings of these effects involve forms of synaptic plasticity that modulates

the efficacy of synaptic transmission. Opioid-mediated synaptic plasticity has been studied extensively in the mesocorticolimbic system in the context of drug addiction (Luscher & Malenka, 2011), and in the dorsal spinal cord in the context of hyperalgesia (Sandkuhler & Gruber-Schoffnegger, 2012). Chronic opioid use elicits epigenetic changes and lasting neural plasticity in the dorsal spinal cord (Sandkuhler & Gruber-Schoffnegger, 2012; Liang *et al.*, 2013; Liang *et al.*, 2014; Chao *et al.*, 2016). Less is known regarding mechanisms whereby opioids influence neural plasticity with acute opioid administration, particularly in motor networks such as the phrenic motor system. Some studies demonstrate that key forms of neuroplasticity such as hippocampal long-term potentiation or depression are sensitive to even a single exposure to opioids (Krug *et al.*, 2001; Wagner *et al.*, 2001; Nugent *et al.*, 2007; Drdla *et al.*, 2009; Dacher & Nugent, 2011). Acute opioid administration leads to synaptic long-term depression in dorsal striatum slices *in vitro* (Atwood *et al.*, 2014), and long-term potentiation in the dorsal spinal cord (Drdla *et al.*, 2009; Zhou *et al.*, 2010). Further investigations concerning mechanisms whereby opioids modulate neuroplasticity is of importance given the high prevalence of opioid prescriptions for pain management.

Here, we aimed to shed further light on the influence of acute opioid use on neuro-adaptive behaviors in the spinal cord by examining the effect of acute morphine delivery on the expression of respiratory motor plasticity. Morphine was chosen for this investigation since 1) morphine reaches significant blood concentrations quickly (~15 minutes); and 2) morphine agonizes mu opioid receptors for ~2 hours at the dose studied here (Hutchinson *et al.*, 2008a). Thus, in the time frame of the present study, the morphine dose used is not expected to elicit persistent mu opioid receptor-induced respiratory depression; nevertheless, downstream pro-inflammatory TLR4 signaling is expected to persist in this time frame (e.g. downstream p38 MAPK phosphorylation; Fig. 9). We did detect morphine and its metabolite M3G in serum samples taken at a time corresponding to the start of neurophysiological recordings. M3G has no affinity for opioid receptors, but does activate TLR4 (Lewis *et al.*, 2010; Doyle & Murphy, 2018). The concentration of morphine in serum (15.5 ± 6 ng/ml) equates to approximately 54 nM. Since brain morphine concentrations are an order of magnitude less than blood concentrations (Xie *et al.*, 1999; Quillinan *et al.*, 2011), measured concentrations are not sufficient to impact respiratory motor output via mu opioid receptor activation (Levitt *et al.*, 2015; Levitt & Williams, 2018). Collectively, serum morphine measurements and the observations that baseline phrenic nerve amplitude and respiratory frequency were similar among all groups are consistent with the interpretation that mu opioid receptor-induced respiratory depression was absent/minimal at the time of our neurophysiological recordings.

Since pLTF was absent >4 hours post-morphine delivery, we suggest off-target mechanisms other than morphine-induced mu opioid receptor activation are responsible for impaired pLTF. Presence of pLTF in morphine-treated rats that received (+)-naloxone demonstrates that TLR4 activation was necessary in the mechanism whereby morphine undermines pLTF. This finding is consistent with predicted pro-inflammatory profiles following TLR4 activation since even mild inflammation triggered by low-dose LPS (a potent TLR4 agonist) abolishes mAIH-induced pLTF in rats (Vinit *et al.*, 2011; Huxtable *et al.*, 2013; Tadjalli *et al.*, 2021). Thus, we predict that drugs that inhibit pro-inflammatory cytokine signaling

(Hocker & Huxtable, 2018) and/or p38 MAP kinase (Huxtable *et al.*, 2015) may restore pLTF following morphine delivery.

To our knowledge, only one other study has examined the effect of acute opioid delivery on respiratory motor plasticity. Ivancev and colleagues (2013) examined the effect of continuous intravenous remifentanil (a short-acting, potent mu opioid agonist) on pLTF expression in rats (Ivancev *et al.*, 2013). The fundamental difference between our study and that of Ivancev and colleagues is that pLTF was suppressed only with continuous infusion of remifentanil. In their study, when remifentanil infusion was stopped at 60-minutes post-AIH, phrenic nerve activity increased above baseline levels, which was interpreted as pLTF. In their study, however, continuous remifentanil infusion suppressed baseline phrenic nerve activity, and time control studies (without AIH) were not performed with remifentanil infusion. Therefore, the rebound increase in phrenic nerve activity following cessation of remifentanil infusion may have been due to removal of continuous mu opioid receptor-induced respiratory depression versus activation of endogenous mechanisms of plasticity (i.e. pLTF). Because of these differences in drug/protocol, it is difficult to compare our studies. Further studies concerning the impact of continuous remifentanil infusion on mAIH-induced pLTF is worthy of investigation.

The ‘inflammation’ of opioid use: mechanisms that impair respiratory motor plasticity

Pioneering work demonstrate that morphine activates the innate immune system and activates glia (Watkins *et al.*, 2005). Others confirmed this finding, implicating inflammation as a potential mechanism for at least some of the opioid side effects (e.g. loss of analgesia, tolerance) (DeLeo *et al.*, 2004; Johnston *et al.*, 2004; Shavit *et al.*, 2005; Watkins *et al.*, 2005; Hutchinson *et al.*, 2011; Due *et al.*, 2012). Morphine activates TLR4, increasing the expression of pro-inflammatory cytokines that can secondarily oppose opioid-induced analgesia (Hutchinson *et al.*, 2008a; Watkins *et al.*, 2009; Ellis *et al.*, 2016). TLR4 antagonists prolong morphine analgesia, suggesting that morphine efficacy may be partially hindered by TLR4-mediated inflammatory signaling (Hutchinson *et al.*, 2010). Since many opioids including morphine, oxycodone, buprenorphine and fentanyl activate TLR4 signaling (Wang *et al.*, 2012), opioid receptor inactive TLR4 inhibitors such as (+)-naloxone may block certain side effects of opioids (Lewis *et al.*, 2010; Lewis *et al.*, 2012).

Although it is not fully understood how morphine activates TLR4 signaling, it may result indirectly from morphine metabolites. Morphine is metabolized primarily into morphine-3-glucuronide (M3G) and morphine-6-glucuronide (M6G) (Coughtrie *et al.*, 1989; Zelcer *et al.*, 2005). M6G is a mu opioid receptor agonist that contributes to morphine analgesic effects; in contrast, M3G has extremely low affinity for opioid receptors (van Dorp *et al.*, 2006), but is a potent activator of TLR4 (Lewis *et al.*, 2010; Due *et al.*, 2012). Since we suggest that morphine suppresses pLTF through TLR4 signaling, anti-inflammatory drugs targeting TLR4 or p38 MAP kinase may prevent at least some unwanted side effects, and enable mechanisms of respiratory plasticity such as pLTF.

In the present study, we explored whether acute morphine delivery blocks mAIH-induced spinal respiratory (phrenic) motor plasticity via mechanisms that require TLR4 signaling. Moderate AIH-induced phrenic motor plasticity represents an important mechanism

to ensure adequate breathing and/or breathing stability (Mahamed & Mitchell, 2007, 2008); 2) has major translational relevance since repetitive AIH is emerging as a novel treatment to restore breathing ability and non-respiratory motor behaviors (e.g. walking) in neuromuscular disorders that compromise movement such as spinal cord injury, ALS and MS (Gonzalez-Rothi *et al.*, 2015; Fuller & Mitchell, 2017); and 3) highly sensitive to inflammation (Huxtable *et al.*, 2013; Agosto-Marlin *et al.*, 2018). Our demonstration that morphine blocks pLTF via a TLR4-dependent mechanism is of importance since it advances our understanding of mechanisms whereby opioids impair control of breathing and further suggests that co-administration of opioids to control pain may thwart the therapeutic efficacy of repetitive AIH since many clinical populations that may benefit from therapeutic AIH often suffer from chronic pain (Finnerup & Baastrup, 2012; Woller & Hook, 2013).

Although the location of the relevant TLR4 receptors was not investigated in this study, TLR4 receptors are expressed in the periphery and at multiple places in the central nervous system, including brainstem and spinal cord respiratory circuits. Since pLTF is induced by serotonin receptor activation on/near phrenic motor neurons within the spinal cord (Tadjalli & Mitchell, 2019), and the resulting plasticity appears to reside within phrenic motor neurons per se (Devinney *et al.*, 2015; Dale *et al.*, 2017), the relevant TLR4 receptors are likely expressed within the region of the phrenic motor nucleus located in the ventral cervical spinal cord. Two lines of evidence support this idea since activation of TLR4 receptors via systemic LPS: 1) undermines pLTF via cervical spinal cytokine signaling (Hocker & Huxtable, 2018); and 2) impairs pLTF via cervical spinal serine-threonine protein phosphatase activity (Tadjalli *et al.*, 2021). Although the hypothesis that systemic morphine impairs pLTF via cervical spinal inflammatory cascades remains to be tested directly, our finding that morphine activates p38 MAPK within cervical spinal microglia is consistent with this hypothesis.

Downstream products of the innate immune response mediated by TLR4 signaling following morphine administration include transcription factors and cytokines. For example, morphine can induce activation of NF-κB and production of proinflammatory cytokines such as IL-1β and TNF-α (Wang *et al.*, 2012; Wang *et al.*, 2016). Furthermore, it has been demonstrated that morphine is able to induce these biological effects via LPS-like interactions with TLR4's co-receptor MD-2 (Wang *et al.*, 2012). Since cytokines such as IL-1β are known to negatively regulate mAIH-induced pLTF (Hocker & Huxtable, 2018), it is possible that deficits in pLTF following morphine could be secondary to IL-1β pro-inflammatory signaling. Although this concept was not tested in the present study, further investigations are warranted to answer this important question.

Morphine-induced modulation of microglial p38 MAPK phosphorylation/activation

We show that a single analgesic dose of morphine results in a rapid biochemical change at the molecular level within the cervical spinal cord. Specifically, morphine exclusively enhanced p38 MAPK phosphorylation/activation within microglia of the ventral cervical spinal segments encompassing the phrenic motor nucleus. Morphine-induced p38 MAPK phosphorylation requires TLR4 signaling since this effect was prevented by pre-treatment

with (+)-naloxone. Thus, even a single morphine dose can rapidly influence cellular networks capable of modulating the expression of phrenic motor plasticity.

The p38 MAPK family is well-known for its role in both promoting and responding to inflammation (Correa & Eales, 2012). p38 MAPK is a key regulator of inflammatory cascades, that include cytokines, chemokines, NF-κB, cyclooxygenase 2 and other proteins, often perpetuating a self-sustaining cycle (Kaminska, 2005; Cuadrado & Nebreda, 2010; Kyriakis & Avruch, 2012). p38 MAPK signaling is also an important regulator of synaptic plasticity (Thomas & Huganir, 2004; Moult *et al.*, 2008; Falcicchia *et al.*, 2020). We provide correlative evidence that morphine upregulates p38 MAPK phosphorylation/activation in spinal microglia, potentially orchestrating relevant cellular cascades that impair mAIH-induced pLTF. This possibility aligns with a prior report demonstrating that cervical spinal p38 MAPK activity undermines mAIH-induced pLTF in the context of neuro-inflammation elicited by one day of severe intermittent hypoxia—a physiologically relevant stimulus mimicking aspects of sleep apnea (Huxtable *et al.*, 2015).

A unique aspect of our findings was that acute morphine enhanced p38 MAPK phosphorylation/activation in spinal CD11b-positive cells: the morphology of phospho-p38 immunoreactive CD11b-positive cells showed small cell bodies with ramified processes, indicative of microglia. To our knowledge, this is the first demonstration of morphine-induced enhancement of microglial p38 MAPK activity in a rapid time scale. Neurons had close contacts with phospho-p38 immunoreactive cells, but co-localization was not observed between phospho-p38 MAPK and NeuN. Morphine-induced p38 MAPK activation is coincident with impaired mAIH-induced pLTF, and reversal of p38 MAPK activation by (+)-naloxone pre-treatment is paralleled by pLTF restoration. Thus, selective microglial p38 MAPK activation via TLR4-dependent mechanisms may be a critical link in morphine-induced deficits in phrenic motor plasticity. This hypothesis awaits direct experimental verification. The proposed mechanisms by which morphine inhibits moderate acute intermittent hypoxia-induced phrenic long-term facilitation is illustrated in figure 10.

Chronic morphine delivery is known to enhance microglial (but not neuronal or astrocytic) p38 MAPK activation coincident with the formation of tolerance (Cui *et al.*, 2006; Wang *et al.*, 2009; Horvath *et al.*, 2010). Spinal inhibition of p38 MAPK activity (Cui *et al.*, 2006; Chen *et al.*, 2008) or spinal intrathecal administration of minocycline, an inhibitor of microglia activation (Cui *et al.*, 2008), attenuated morphine-induced tolerance. These findings indicate that activation of microglial MAPKs, particularly the p38 family, is critical to the development of some of the negative side effects of morphine analgesia (e.g. tolerance). While spinal MAPK involvement in tolerance and hyperalgesia following chronic morphine delivery is well documented, studies evaluating the short-term effects of acute morphine administration on p38 MAPK activity have been lacking. To the best of our knowledge, our study is the first to address this knowledge gap, illustrating that a single systemic administration of morphine (within a few hours) also enhances p38 MAPK activity exclusively in microglia. Understandings the early-onset mechanisms by which opioids influence neural network activity might facilitate development of therapeutic approaches to combat unfavorable opioid side-effects. This has been an important and enduring notion in pain management, not least because the soaring increase in opioid prescriptions for the

treatment of acute pain is thought to be an important predictor/driver of persistent opioid use and addiction (Calcaterra *et al.*, 2016; Sun *et al.*, 2016; Brummett *et al.*, 2017; Stark *et al.*, 2017).

Impaired phrenic responses during chemoreflex activation: TLR4 effects

Diminishing reflex responses to changes in O_2 and CO_2 levels undermines the ability of the ventilatory control system to compensate for pathologies that compromise adequate lung ventilation. Opioids are widely known to suppress hypoxic and hypercapnic ventilatory responses in humans and animal models (Kirby & McQueen, 1986; Bailey *et al.*, 2000; Dahan *et al.*, 2001; Romberg *et al.*, 2003; Modalen *et al.*, 2006; Zhang *et al.*, 2007, 2009; Zhang *et al.*, 2011; May *et al.*, 2013). Although these effects are assumed to arise from mu opioid receptor activation, our data suggest additional effects may arise from TLR4 activation. The morphine dose and timing of experiments in this study reflect the TLR4 versus mu opioid receptor actions due to the short half-life of morphine. Although differences in the short-term hypoxic phrenic response (Fig. 2B) were minimal among groups, responses to maximal chemoreflex activation with hypoxic hypercapnia were blunted in morphine-treated rats (Fig. 8). This finding suggests that morphine diminished the capacity (versus sensitivity) of phrenic (and ventilatory) responses to maximum chemoreflex activation (10% O_2/7% inspired CO_2). Since these data were collected at the end of experiments, when mu opioid receptors were no longer activated, and the effects were prevented by (+)-naloxone pretreatment, morphine appears to impair maximal phrenic responses to chemoreflex activation via TLR4 activation.

To date few studies have reported effects of inflammation on respiratory chemoreflexes (for review refer to (Huxtable *et al.*, 2011)). Majority of the reports examined the impact of systemic inflammation on hypoxic ventilatory responses, with only one study examining the impact of systemic LPS (TLR4 agonist) on maximal chemoreflex stimulation (10.5% inspired O2 with 7% inspired CO2 / balance N2) of breathing. As demonstrated by Huxtable and colleagues (2011), there is evidence to suggest that LPS-induced inflammation reduces ventilation during maximal chemoreceptor stimulation. The precise mechanisms by which inflammation reduces max chemoreceptor stimulation of breathing was not investigated. Our findings in the present study conceptually agree with the report that max chemoreflex responses can be blunted in conditions where inflammatory processes are present. We extend this notion by demonstrating that max chemoreflex stimulation of respiratory activity (as measured by phrenic nerve motor output) is restored in rats that received the TLR4 inhibitor before morphine. We are unsure exactly which central sites are being affected by inflammatory processes; their identification was beyond the scope of this study. Overall, our data suggests that downregulation of chemoreflexes by immune driven inflammatory processes secondary to opioid use should be taken into consideration in patients with unstable ventilatory chemoreflex control.

Supplementary Material

Refer to Web version on PubMed Central for supplementary material.

Acknowledgments

Funding: Supported by National Institutes of Health SPARC Initiative (OT2 OD023854; GSM, DCB, ESL); National Institute on Drug Abuse (R01 DA047978; ESL); NIH National Center for Advancing Translational Sciences (UL1TR001427; CRM); Parker B. Francis Family Foundation Fellowship Grant (AT).

Data Availably Statement:

The data that support the findings of this study are available from the corresponding author upon reasonable request.

Author Profile:

Arash Tadjalli obtained his PhD from the Department of Cell and Systems Biology at the University of Toronto, Canada, where he studied the mechanisms of neuroplasticity in brainstem circuits that regulate upper airway motor activity *in vivo*. As a Francis Family Foundation Fellow at the University of Florida, he is currently studying mechanisms of neuro-glia interactions in giving rise to spinal respiratory motor plasticity in the healthy brain, as well as in disease states characterized by neuroinflammation.

REFERENCES

Agosto-Marlin IM, Nichols NL & Mitchell GS. (2018). Systemic inflammation inhibits serotonin receptor 2-induced phrenic motor facilitation upstream from BDNF/TrkB signaling. Journal of neurophysiology 119, 2176–2185. [PubMed: 29513151]

Araldi D, Bogen O, Green PG & Levine JD. (2019). Role of Nociceptor Toll-like Receptor 4 (TLR4) in Opioid-Induced Hyperalgesia and Hyperalgesic Priming. The Journal of neuroscience : the official journal of the Society for Neuroscience 39, 6414–6424. [PubMed: 31209174]

Atwood BK, Kupferschmidt DA & Lovinger DM. (2014). Opioids induce dissociable forms of long-term depression of excitatory inputs to the dorsal striatum. Nat Neurosci 17, 540–548. [PubMed: 24561996]

Bachmutsky I, Wei XP, Kish E & Yackle K. (2020). Opioids depress breathing through two small brainstem sites. Elife 9.

Bailey PL, Lu JK, Pace NL, Orr JA, White JL, Hamber EA, Slawson MH, Crouch DJ & Rollins DE. (2000). Effects of intrathecal morphine on the ventilatory response to hypoxia. N Engl J Med 343, 1228–1234. [PubMed: 11071674]

Baker-Herman TL, Fuller DD, Bavis RW, Zabka AG, Golder FJ, Doperalski NJ, Johnson RA, Watters JJ & Mitchell GS. (2004). BDNF is necessary and sufficient for spinal respiratory plasticity following intermittent hypoxia. Nat Neurosci 7, 48–55. [PubMed: 14699417]

Baker-Herman TL & Mitchell GS. (2002). Phrenic long-term facilitation requires spinal serotonin receptor activation and protein synthesis. The Journal of neuroscience : the official journal of the Society for Neuroscience 22, 6239–6246. [PubMed: 12122082]

Berterame S, Erthal J, Thomas J, Fellner S, Vosse B, Clare P, Hao W, Johnson DT, Mohar A, Pavadia J, Samak AK, Sipp W, Sumyai V, Suryawati S, Toufiq J, Yans R & Mattick RP. (2016). Use of and barriers to access to opioid analgesics: a worldwide, regional, and national study. Lancet 387, 1644–1656. [PubMed: 26852264]

Boom M, Niesters M, Sarton E, Aarts L, Smith TW & Dahan A. (2012). Non-analgesic effects of opioids: opioid-induced respiratory depression. Curr Pharm Des 18, 5994–6004. [PubMed: 22747535]

Brummett CM, Waljee JF, Goesling J, Moser S, Lin P, Englesbe MJ, Bohnert ASB, Kheterpal S & Nallamothu BK. (2017). New Persistent Opioid Use After Minor and Major Surgical Procedures in US Adults. JAMA Surg 152, e170504. [PubMed: 28403427]

Calcaterra SL, Yamashita TE, Min SJ, Keniston A, Frank JW & Binswanger IA. (2016). Opioid Prescribing at Hospital Discharge Contributes to Chronic Opioid Use. J Gen Intern Med 31, 478–485. [PubMed: 26553336]

Chao YC, Xie F, Li X, Guo R, Yang N, Zhang C, Shi R, Guan Y, Yue Y & Wang Y. (2016). Demethylation regulation of BDNF gene expression in dorsal root ganglion neurons is implicated in opioid-induced pain hypersensitivity in rats. Neurochem Int 97, 91–98. [PubMed: 26970395]

Chen Y, Geis C & Sommer C. (2008). Activation of TRPV1 contributes to morphine tolerance: involvement of the mitogen-activated protein kinase signaling pathway. The Journal of neuroscience : the official journal of the Society for Neuroscience 28, 5836–5845. [PubMed: 18509045]

Chen Y & Sommer C. (2009). The role of mitogen-activated protein kinase (MAPK) in morphine tolerance and dependence. Mol Neurobiol 40, 101–107. [PubMed: 19468867]

Chin PY, Dorian CL, Hutchinson MR, Olson DM, Rice KC, Moldenhauer LM & Robertson SA. (2016). Novel Toll-like receptor-4 antagonist (+)-naloxone protects mice from inflammation-induced preterm birth. Sci Rep 6, 36112. [PubMed: 27819333]

Christ A, Arranto CA, Schindler C, Klima T, Hunziker PR, Siegemund M, Marsch SC, Eriksson U & Mueller C. (2006). Incidence, risk factors, and outcome of aspiration pneumonitis in ICU overdose patients. Intensive Care Med 32, 1423–1427. [PubMed: 16826384]

Christrup LL. (1997). Morphine metabolites. Acta Anaesthesiol Scand41, 116–122. [PubMed: 9061094]

Collingridge GL, Peineau S, Howland JG & Wang YT. (2010). Long-term depression in the CNS. Nature reviews Neuroscience 11, 459–473. [PubMed: 20559335]

Correa SA & Eales KL. (2012). The Role of p38 MAPK and Its Substrates in Neuronal Plasticity and Neurodegenerative Disease. J Signal Transduct 2012, 649079. [PubMed: 22792454]

Coughtrie MW, Ask B, Rane A, Burchell B & Hume R. (1989). The enantioselective glucuronidation of morphine in rats and humans. Evidence for the involvement of more than one UDP-glucuronosyltransferase isoenzyme. Biochem Pharmacol 38, 3273–3280. [PubMed: 2510730]

Cuadrado A & Nebreda AR. (2010). Mechanisms and functions of p38 MAPK signalling. Biochem J 429, 403–417. [PubMed: 20626350]

Cui Y, Chen Y, Zhi JL, Guo RX, Feng JQ & Chen PX. (2006). Activation of p38 mitogen-activated protein kinase in spinal microglia mediates morphine antinociceptive tolerance. Brain research 1069, 235–243. [PubMed: 16403466]

Cui Y, Liao XX, Liu W, Guo RX, Wu ZZ, Zhao CM, Chen PX & Feng JQ. (2008). A novel role of minocycline: attenuating morphine antinociceptive tolerance by inhibition of p38 MAPK in the activated spinal microglia. Brain Behav Immun 22, 114–123. [PubMed: 17919885]

Dacher M & Nugent FS. (2011). Morphine-induced modulation of LTD at GABAergic synapses in the ventral tegmental area. Neuropharmacology 61, 1166–1171. [PubMed: 21129388]

Dahan A, Sarton E, Teppema L, Olievier C, Nieuwenhuijs D, Matthes HW & Kieffer BL. (2001). Anesthetic potency and influence of morphine and sevoflurane on respiration in mu-opioid receptor knockout mice. Anesthesiology 94, 824–832. [PubMed: 11388534]

Dale EA, Fields DP, Devinney MJ & Mitchell GS. (2017). Phrenic motor neuron TrkB expression is necessary for acute intermittent hypoxia-induced phrenic long-term facilitation. Experimental neurology 287, 130–136. [PubMed: 27185271]

de Freitas BG, Pereira LM, Santa-Cecilia FV, Hosch NG, Picolo G, Cury Y & Zambelli VO. (2019). Mitogen-Activated Protein Kinase Signaling Mediates Morphine Induced-Delayed Hyperalgesia. Front Neurosci 13, 1018. [PubMed: 31616243]

DeLeo JA, Tanga FY & Tawfik VL. (2004). Neuroimmune activation and neuroinflammation in chronic pain and opioid tolerance/hyperalgesia. Neuroscientist 10, 40–52. [PubMed: 14987447]

Deng M, Chen SR, Chen H, Luo Y, Dong Y & Pan HL. (2019). Mitogen-activated protein kinase signaling mediates opioid-induced presynaptic NMDA receptor activation and analgesic tolerance. Journal of neurochemistry 148, 275–290. [PubMed: 30444263]

Devinney MJ, Fields DP, Huxtable AG, Peterson TJ, Dale EA & Mitchell GS. (2015). Phrenic long-term facilitation requires PKCtheta activity within phrenic motor neurons. The Journal of neuroscience : the official journal of the Society for Neuroscience 35, 8107–8117. [PubMed: 26019328]

Devinney MJ, Huxtable AG, Nichols NL & Mitchell GS. (2013). Hypoxia-induced phrenic long-term facilitation: emergent properties. Annals of the New York Academy of Sciences 1279, 143–153. [PubMed: 23531012]

Dowell D, Haegerich TM & Chou R. (2016). CDC Guideline for Prescribing Opioids for Chronic Pain - United States, 2016. MMWR Recomm Rep 65, 1–49.

Doyle HH & Murphy AZ. (2018). Sex-dependent influences of morphine and its metabolites on pain sensitivity in the rat. Physiol Behav 187, 32–41. [PubMed: 29199028]

Drdla R, Gassner M, Gingl E & Sandkuhler J. (2009). Induction of synaptic long-term potentiation after opioid withdrawal. Science 325, 207–210. [PubMed: 19590003]

Due MR, Piekarz AD, Wilson N, Feldman P, Ripsch MS, Chavez S, Yin H, Khanna R & White FA. (2012). Neuroexcitatory effects of morphine-3-glucuronide are dependent on Toll-like receptor 4 signaling. J Neuroinflammation 9, 200. [PubMed: 22898544]

Eidson LN, Inoue K, Young LJ, Tansey MG & Murphy AZ. (2017). Toll-like Receptor 4 Mediates Morphine-Induced Neuroinflammation and Tolerance via Soluble Tumor Necrosis Factor Signaling. Neuropsychopharmacology 42, 661–670. [PubMed: 27461080]

Eidson LN & Murphy AZ. (2013). Blockade of Toll-like receptor 4 attenuates morphine tolerance and facilitates the pain relieving properties of morphine. The Journal of neuroscience : the official journal of the Society for Neuroscience 33, 15952–15963. [PubMed: 24089500]

Eldridge FL. (1976). Quantification of electrical activity in the phrenic nerve in the study of ventilatory control. Chest70, 154–157. [PubMed: 939134]

Ellis A, Grace PM, Wieseler J, Favret J, Springer K, Skarda B, Ayala M, Hutchinson MR, Falci S, Rice KC, Maier SF & Watkins LR. (2016). Morphine amplifies mechanical allodynia via TLR4 in a rat model of spinal cord injury. Brain Behav Immun 58, 348–356. [PubMed: 27519154]

Falcicchia C, Tozzi F, Arancio O, Watterson DM & Origlia N. (2020). Involvement of p38 MAPK in Synaptic Function and Dysfunction. Int J Mol Sci 21.

Farney RJ, Walker JM, Cloward TV & Rhondeau S. (2003). Sleep-disordered breathing associated with long-term opioid therapy. Chest 123, 632–639. [PubMed: 12576394]

Finnerup NB & Baastrup C. (2012). Spinal cord injury pain: mechanisms and management. Curr Pain Headache Rep 16, 207–216. [PubMed: 22392531]

Fuller DD, Bach KB, Baker TL, Kinkead R & Mitchell GS. (2000). Long term facilitation of phrenic motor output. Respiration physiology 121, 135–146. [PubMed: 10963770]

Fuller DD, Johnson SM, Olson EB Jr. & Mitchell GS. (2003). Synaptic pathways to phrenic motoneurons are enhanced by chronic intermittent hypoxia after cervical spinal cord injury. The Journal of neuroscience : the official journal of the Society for Neuroscience 23, 2993–3000. [PubMed: 12684486]

Fuller DD & Mitchell GS. (2017). Respiratory neuroplasticity - Overview, significance and future directions. Experimental neurology 287, 144–152. [PubMed: 27208699]

Golder FJ & Mitchell GS. (2005). Spinal synaptic enhancement with acute intermittent hypoxia improves respiratory function after chronic cervical spinal cord injury. The Journal of neuroscience : the official journal of the Society for Neuroscience 25, 2925–2932. [PubMed: 15772352]

Gonzalez-Rothi EJ, Lee KZ, Dale EA, Reier PJ, Mitchell GS & Fuller DD. (2015). Intermittent hypoxia and neurorehabilitation. Journal of applied physiology 119, 1455–1465. [PubMed: 25997947]

Grundy D (2015). Principles and standards for reporting animal experiments in The Journal of Physiology and Experimental Physiology. J Physiol, 593: 2547–2549. [PubMed: 26095019]

Gulur P, Williams L, Chaudhary S, Koury K & Jaff M. (2014). Opioid tolerance--a predictor of increased length of stay and higher readmission rates. Pain Physician 17, E503–507. [PubMed: 25054400]

Hajiha M, DuBord MA, Liu H & Horner RL. (2009). Opioid receptor mechanisms at the hypoglossal motor pool and effects on tongue muscle activity in vivo. The Journal of physiology 587, 2677–2692. [PubMed: 19403616]

Hocker AD & Huxtable AG. (2018). IL-1 receptor activation undermines respiratory motor plasticity after systemic inflammation. Journal of applied physiology 125, 504–512. [PubMed: 29565772]

Hoffman MS, Nichols NL, Macfarlane PM & Mitchell GS. (2012). Phrenic long-term facilitation after acute intermittent hypoxia requires spinal ERK activation but not TrkB synthesis. Journal of applied physiology 113, 1184–1193. [PubMed: 22961271]

Horvath RJ, Landry RP, Romero-Sandoval EA & DeLeo JA. (2010). Morphine tolerance attenuates the resolution of postoperative pain and enhances spinal microglial p38 and extracellular receptor kinase phosphorylation. Neuroscience 169, 843–854. [PubMed: 20493931]

Hutchinson MR, Coats BD, Lewis SS, Zhang Y, Sprunger DB, Rezvani N, Baker EM, Jekich BM, Wieseler JL, Somogyi AA, Martin D, Poole S, Judd CM, Maier SF & Watkins LR. (2008a). Proinflammatory cytokines oppose opioid-induced acute and chronic analgesia. Brain Behav Immun 22, 1178–1189. [PubMed: 18599265]

Hutchinson MR, Shavit Y, Grace PM, Rice KC, Maier SF & Watkins LR. (2011). Exploring the neuroimmunopharmacology of opioids: an integrative review of mechanisms of central immune signaling and their implications for opioid analgesia. Pharmacol Rev 63, 772–810. [PubMed: 21752874]

Hutchinson MR, Zhang Y, Brown K, Coats BD, Shridhar M, Sholar PW, Patel SJ, Crysdale NY, Harrison JA, Maier SF, Rice KC & Watkins LR. (2008b). Non-stereoselective reversal of neuropathic pain by naloxone and naltrexone: involvement of toll-like receptor 4 (TLR4). Eur J Neurosci 28, 20–29. [PubMed: 18662331]

Hutchinson MR, Zhang Y, Shridhar M, Evans JH, Buchanan MM, Zhao TX, Slivka PF, Coats BD, Rezvani N, Wieseler J, Hughes TS, Landgraf KE, Chan S, Fong S, Phipps S, Falke JJ, Leinwand LA, Maier SF, Yin H, Rice KC & Watkins LR. (2010). Evidence that opioids may have toll-like receptor 4 and MD-2 effects. Brain Behav Immun 24, 83–95. [PubMed: 19679181]

Huxtable AG, Smith SM, Peterson TJ, Watters JJ & Mitchell GS. (2015). Intermittent Hypoxia-Induced Spinal Inflammation Impairs Respiratory Motor Plasticity by a Spinal p38 MAP Kinase-Dependent Mechanism. The Journal of neuroscience : the official journal of the Society for Neuroscience 35, 6871–6880. [PubMed: 25926462]

Huxtable AG, Smith SM, Vinit S, Watters JJ & Mitchell GS. (2013). Systemic LPS induces spinal inflammatory gene expression and impairs phrenic long-term facilitation following acute intermittent hypoxia. Journal of applied physiology 114, 879–887. [PubMed: 23329821]

Huxtable AG, Vinit S, Windelborn JA, Crader SM, Guenther CH, Watters JJ & Mitchell GS. (2011). Systemic inflammation impairs respiratory chemoreflexes and plasticity. Respiratory physiology & neurobiology 178, 482–489. [PubMed: 21729770]

Iijima I, Minamikawa J, Jacobson AE, Brossi A & Rice KC. (1978). Studies in the (+)-morphinan series. 5. Synthesis and biological properties of (+)-naloxone. J Med Chem 21, 398–400. [PubMed: 206698]

Ivancev B, Carev M, Pecotic R, Valic M, Pavlinac Dodig I, Karanovic N & Dogas Z. (2013). Remifentanil reversibly abolished phrenic long term facilitation in rats subjected to acute intermittent hypoxia. J Physiol Pharmacol 64, 485–492. [PubMed: 24101395]

Johnston IN, Milligan ED, Wieseler-Frank J, Frank MG, Zapata V, Campisi J, Langer S, Martin D, Green P, Fleshner M, Leinwand L, Maier SF & Watkins LR. (2004). A role for proinflammatory cytokines and fractalkine in analgesia, tolerance, and subsequent pain facilitation induced by chronic intrathecal morphine. The Journal of neuroscience : the official journal of the Society for Neuroscience 24, 7353–7365. [PubMed: 15317861]

Kaminska B (2005). MAPK signalling pathways as molecular targets for anti-inflammatory therapy--from molecular mechanisms to therapeutic benefits. Biochim Biophys Acta 1754, 253–262. [PubMed: 16198162]

Kirby GC & McQueen DS. (1986). Characterization of opioid receptors in the cat carotid body involved in chemosensory depression in vivo. Br J Pharmacol 88, 889–898. [PubMed: 2874862]

Krug M, Brodemann R & Wagner M. (2001). Simultaneous activation and opioid modulation of long-term potentiation in the dentate gyrus and the hippocampal CA3 region after stimulation of the perforant pathway in freely moving rats. Brain research 913, 68–77. [PubMed: 11532248]

Kuo CK, Hanioka N, Hoshikawa Y, Oguri K & Yoshimura H. (1991). Species difference of site-selective glucuronidation of morphine. J Pharmacobiodyn 14, 187–193. [PubMed: 1941499]

Kyriakis JM & Avruch J. (2012). Mammalian MAPK signal transduction pathways activated by stress and inflammation: a 10-year update. Physiol Rev 92, 689–737. [PubMed: 22535895]

Labella FS, Pinsky C & Havlicek V. (1979). Morphine derivatives with diminished opiate receptor potency show enhanced central excitatory activity. Brain research 174, 263–271. [PubMed: 226219]

Levitt ES, Abdala AP, Paton JF, Bissonnette JM & Williams JT. (2015). mu opioid receptor activation hyperpolarizes respiratory-controlling Kolliker-Fuse neurons and suppresses post-inspiratory drive. The Journal of physiology 593, 4453–4469. [PubMed: 26175072]

Levitt ES & Williams JT. (2018). Desensitization and Tolerance of Mu Opioid Receptors on Pontine Kolliker-Fuse Neurons. Mol Pharmacol 93, 8–13. [PubMed: 29097440]

Lewis SS, Hutchinson MR, Rezvani N, Loram LC, Zhang Y, Maier SF, Rice KC & Watkins LR. (2010). Evidence that intrathecal morphine-3-glucuronide may cause pain enhancement via toll-like receptor 4/MD-2 and interleukin-1beta. Neuroscience 165, 569–583. [PubMed: 19833175]

Lewis SS, Loram LC, Hutchinson MR, Li CM, Zhang Y, Maier SF, Huang Y, Rice KC & Watkins LR. (2012). (+)-naloxone, an opioid-inactive toll-like receptor 4 signaling inhibitor, reverses multiple models of chronic neuropathic pain in rats. J Pain 13, 498–506. [PubMed: 22520687]

Liang DY, Li X & Clark JD. (2013). Epigenetic regulation of opioid-induced hyperalgesia, dependence, and tolerance in mice. J Pain 14, 36–47. [PubMed: 23273833]

Liang DY, Sun Y, Shi XY, Sahbaie P & Clark JD. (2014). Epigenetic regulation of spinal cord gene expression controls opioid-induced hyperalgesia. Mol Pain 10, 59. [PubMed: 25217253]

Luscher C & Malenka RC. (2011). Drug-evoked synaptic plasticity in addiction: from molecular changes to circuit remodeling. Neuron 69, 650–663. [PubMed: 21338877]

MacFarlane PM, Satriotomo I, Windelborn JA & Mitchell GS. (2009). NADPH oxidase activity is necessary for acute intermittent hypoxia-induced phrenic long-term facilitation. The Journal of physiology 587, 1931–1942. [PubMed: 19237427]

Mahamed S & Mitchell GS. (2007). Is there a link between intermittent hypoxia-induced respiratory plasticity and obstructive sleep apnoea? Exp Physiol 92, 27–37. [PubMed: 17099064]

Mahamed S & Mitchell GS. (2008). Simulated apnoeas induce serotonin-dependent respiratory long-term facilitation in rats. The Journal of physiology 586, 2171–2181. [PubMed: 18292130]

May WJ, Gruber RB, Discala JF, Puskovic V, Henderson F, Palmer LA & Lewis SJ. (2013). Morphine has latent deleterious effects on the ventilatory responses to a hypoxic challenge. Open J Mol Integr Physiol 3, 166–180. [PubMed: 25045593]

McGuire M, Zhang Y, White DP & Ling L. (2003). Chronic intermittent hypoxia enhances ventilatory long-term facilitation in awake rats. Journal of applied physiology 95, 1499–1508. [PubMed: 12819226]

Mitchell GS & Johnson SM. (2003). Neuroplasticity in respiratory motor control. Journal of applied physiology 94, 358–374. [PubMed: 12486024]

Modalen AO, Quiding H, Frey J, Westman L & Lindahl S. (2006). A novel molecule with peripheral opioid properties: the effects on hypercarbic and hypoxic ventilation at steady-state compared with morphine and placebo. Anesth Analg 102, 104–109. [PubMed: 16368813]

Montandon G & Horner R. (2014). CrossTalk proposal: The preBotzinger complex is essential for the respiratory depression following systemic administration of opioid analgesics. The Journal of physiology 592, 1159–1162. [PubMed: 24634011]

Moult PR, Correa SA, Collingridge GL, Fitzjohn SM & Bashir ZI. (2008). Co-activation of p38 mitogen-activated protein kinase and protein tyrosine phosphatase underlies metabotropic glutamate receptor-dependent long-term depression. The Journal of physiology 586, 2499–2510. [PubMed: 18356198]

Nugent FS, Penick EC & Kauer JA. (2007). Opioids block long-term potentiation of inhibitory synapses. Nature 446, 1086–1090. [PubMed: 17460674]

Palkovic B, Marchenko V, Zuperku EJ, Stuth EAE & Stucke AG. (2020). Multi-Level Regulation of Opioid-Induced Respiratory Depression. Physiology (Bethesda) 35, 391–404. [PubMed: 33052772]

Pattinson KT. (2008). Opioids and the control of respiration. Br J Anaesth100, 747–758. [PubMed: 18456641]

Quillinan N, Lau EK, Virk M, von Zastrow M & Williams JT. (2011). Recovery from mu-opioid receptor desensitization after chronic treatment with morphine and methadone. The Journal of neuroscience : the official journal of the Society for Neuroscience 31, 4434–4443. [PubMed: 21430144]

Raghavendra V, Rutkowski MD & DeLeo JA. (2002). The role of spinal neuroimmune activation in morphine tolerance/hyperalgesia in neuropathic and sham-operated rats. The Journal of neuroscience : the official journal of the Society for Neuroscience 22, 9980–9989. [PubMed: 12427855]

Romberg R, Olofsen E, Sarton E, Teppema L & Dahan A. (2003). Pharmacodynamic effect of morphine-6-glucuronide versus morphine on hypoxic and hypercapnic breathing in healthy volunteers. Anesthesiology 99, 788–798. [PubMed: 14508308]

Sandkuhler J & Gruber-Schoffnegger D. (2012). Hyperalgesia by synaptic long-term potentiation (LTP): an update. Curr Opin Pharmacol 12, 18–27. [PubMed: 22078436]

Savilampi J, Ahlstrand R, Magnuson A, Geijer H & Wattwil M. (2014). Aspiration induced by remifentanil: a double-blind, randomized, crossover study in healthy volunteers. Anesthesiology 121, 52–58. [PubMed: 24598216]

Savilampi J, Ahlstrand R, Magnuson A & Wattwil M. (2013). Effects of remifentanil on the esophagogastric junction and swallowing. Acta Anaesthesiol Scand 57, 1002–1009. [PubMed: 23713743]

Seven YB, Perim RR, Hobson OR, Simon AK, Tadjalli A & Mitchell GS. (2018). Phrenic motor neuron adenosine 2A receptors elicit phrenic motor facilitation. The Journal of physiology 596, 1501–1512. [PubMed: 29388230]

Shavit Y, Wolf G, Goshen I, Livshits D & Yirmiya R. (2005). Interleukin-1 antagonizes morphine analgesia and underlies morphine tolerance. Pain 115, 50–59. [PubMed: 15836969]

Stark N, Kerr S & Stevens J. (2017). Prevalence and predictors of persistent post-surgical opioid use: a prospective observational cohort study. Anaesth Intensive Care 45, 700–706. [PubMed: 29137580]

Sun EC, Darnall BD, Baker LC & Mackey S. (2016). Incidence of and Risk Factors for Chronic Opioid Use Among Opioid-Naive Patients in the Postoperative Period. JAMA Intern Med 176, 1286–1293. [PubMed: 27400458]

Tadjalli A & Mitchell GS. (2019). Cervical spinal 5-HT2A and 5-HT2B receptors are both necessary for moderate acute intermittent hypoxia-induced phrenic long-term facilitation. Journal of applied physiology 127, 432–443. [PubMed: 31219768]

Tadjalli A, Seven YB, Perim RR & Mitchell GS. (2021). Systemic inflammation suppresses spinal respiratory motor plasticity via mechanisms that require serine/threonine protein phosphatase activity. J Neuroinflammation 18, 28. [PubMed: 33468163]

Tanda G, Mereu M, Hiranita T, Quarterman JC, Coggiano M & Katz JL. (2016). Lack of Specific Involvement of (+)-Naloxone and (+)-Naltrexone on the Reinforcing and Neurochemical Effects of Cocaine and Opioids. Neuropsychopharmacology 41, 2772–2781. [PubMed: 27296151]

Thomas GM & Huganir RL. (2004). MAPK cascade signalling and synaptic plasticity. Nature reviews Neuroscience 5, 173–183. [PubMed: 14976517]

Valentino RJ, Katz JL, Medzihradsky F & Woods JH. (1983). Receptor binding, antagonist, and withdrawal precipitating properties of opiate antagonists. Life Sci 32, 2887–2896. [PubMed: 6304445]

van Dorp EL, Romberg R, Sarton E, Bovill JG & Dahan A. (2006). Morphine-6-glucuronide: morphine's successor for postoperative pain relief? Anesth Analg 102, 1789–1797. [PubMed: 16717327]

Van Ryswyk E & Antic NA. (2016). Opioids and Sleep-Disordered Breathing. Chest 150, 934–944. [PubMed: 27262224]

Varga AG, Reid BT, Kieffer BL & Levitt ES. (2020). Differential impact of two critical respiratory centres in opioid-induced respiratory depression in awake mice. The Journal of physiology 598, 189–205. [PubMed: 31589332]

Vinit S, Windelborn JA & Mitchell GS. (2011). Lipopolysaccharide attenuates phrenic long-term facilitation following acute intermittent hypoxia. Respiratory physiology & neurobiology 176, 130–135. [PubMed: 21334467]

Volkow ND & Collins FS. (2017). The Role of Science in Addressing the Opioid Crisis. N Engl J Med 377, 391–394. [PubMed: 28564549]

Wagner JJ, Etemad LR & Thompson AM. (2001). Opioid-mediated facilitation of long-term depression in rat hippocampus. J Pharmacol Exp Ther 296, 776–781. [PubMed: 11181906]

Wang X, Loram LC, Ramos K, de Jesus AJ, Thomas J, Cheng K, Reddy A, Somogyi AA, Hutchinson MR, Watkins LR & Yin H. (2012). Morphine activates neuroinflammation in a manner parallel to endotoxin. Proc Natl Acad Sci U S A 109, 6325–6330. [PubMed: 22474354]

Wang X, Zhang Y, Peng Y, Hutchinson MR, Rice KC, Yin H & Watkins LR. (2016). Pharmacological characterization of the opioid inactive isomers (+)-naltrexone and (+)-naloxone as antagonists of toll-like receptor 4. Br J Pharmacol 173, 856–869. [PubMed: 26603732]

Wang Z, Ma W, Chabot JG & Quirion R. (2009). Cell-type specific activation of p38 and ERK mediates calcitonin gene-related peptide involvement in tolerance to morphine-induced analgesia. FASEB J 23, 2576–2586. [PubMed: 19299480]

Watkins LR, Hutchinson MR, Johnston IN & Maier SF. (2005). Glia: novel counter-regulators of opioid analgesia. Trends Neurosci 28, 661–669. [PubMed: 16246435]

Watkins LR, Hutchinson MR, Rice KC & Maier SF. (2009). The “toll” of opioid-induced glial activation: improving the clinical efficacy of opioids by targeting glia. Trends Pharmacol Sci 30, 581–591. [PubMed: 19762094]

Winters BL, Gregoriou GC, Kissiwaa SA, Wells OA, Medagoda DI, Hermes SM, Burford NT, Alt A, Aicher SA & Bagley EE. (2017). Endogenous opioids regulate moment-to-moment neuronal communication and excitability. Nat Commun 8, 14611. [PubMed: 28327612]

Woller SA & Hook MA. (2013). Opioid administration following spinal cord injury: implications for pain and locomotor recovery. Experimental neurology 247, 328–341. [PubMed: 23501709]

Xie R, Hammarlund-Udenaes M, de Boer AG & de Lange EC. (1999). The role of P-glycoprotein in blood-brain barrier transport of morphine: transcortical microdialysis studies in mdr1a (−/−) and mdr1a (+/+) mice. Br J Pharmacol 128, 563–568. [PubMed: 10516633]

Zelcer N, van de Wetering K, Hillebrand M, Sarton E, Kuil A, Wielinga PR, Tephly T, Dahan A, Beijnen JH & Borst P. (2005). Mice lacking multidrug resistance protein 3 show altered morphine pharmacokinetics and morphine-6-glucuronide antinociception. Proc Natl Acad Sci U S A 102, 7274–7279. [PubMed: 15886284]

Zhang Z, Xu F, Zhang C & Liang X. (2007). Activation of opioid mu receptors in caudal medullary raphe region inhibits the ventilatory response to hypercapnia in anesthetized rats. Anesthesiology 107, 288–297. [PubMed: 17667574]

Zhang Z, Xu F, Zhang C & Liang X. (2009). Opioid mu-receptors in medullary raphe region affect the hypoxic ventilation in anesthetized rats. Respiratory physiology & neurobiology 168, 281–288. [PubMed: 19632358]

Zhang Z, Zhuang J, Zhang C & Xu F. (2011). Activation of opioid mu-receptors in the commissural subdivision of the nucleus tractus solitarius abolishes the ventilatory response to hypoxia in anesthetized rats. Anesthesiology 115, 353–363. [PubMed: 21716092]

Zhou HY, Chen SR, Chen H & Pan HL. (2010). Opioid-induced long-term potentiation in the spinal cord is a presynaptic event. The Journal of neuroscience : the official journal of the Society for Neuroscience 30, 4460–4466. [PubMed: 20335482]

Zwicker JD, Zhang Y, Ren J, Hutchinson MR, Rice KC, Watkins LR, Greer JJ & Funk GD. (2014). Glial TLR4 signaling does not contribute to opioid-induced depression of respiration. Journal of applied physiology 117, 857–868. [PubMed: 25103966]

Key Points Summary

- While respiratory complications following opioid use are mainly mediated via activation of mu opioid receptors, long-latency off-target signaling via innate immune toll like receptor 4 (TLR4) may impair other essential elements of breathing control such as respiratory motor plasticity.
- In adult rats, pre-treatment with a single dose of morphine blocked long-term facilitation (LTF) of phrenic motor output via a long-latency TLR4-dependent mechanism.
- In the phrenic motor nucleus, morphine triggered TLR4-dependent activation of microglial p38 MAPK — a key enzyme that orchestrates inflammatory signaling and is known to undermine phrenic LTF.
- Morphine-induced LTF loss may de-stabilize breathing, potentially contributing to respiratory side effects. Therefore, we suggest minimizing TLR-4 signaling may improve breathing stability during opioid therapy.

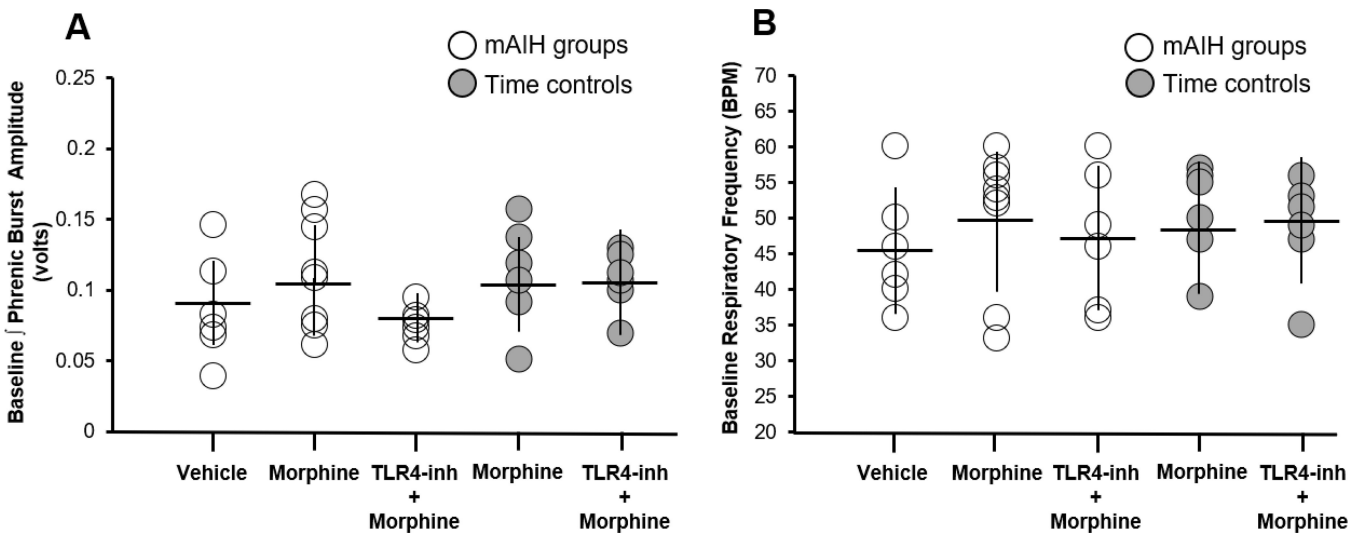

Figure 1. Baseline inspiratory phrenic burst amplitude and baseline respiratory frequency in different treatment groups.

A and **B**, Group data showing that baseline phrenic nerve inspiratory burst amplitudes (A) and respiratory frequency (B) were similar in all treatment groups. Solid horizontal line within each data series indicates average group mean, and the vertical bar protruding above and below the horizontal line indicates standard deviation for each data set. Circles indicate individual data points in each experimental group. BPM: breaths per minute; TLR4-inh: TLR4 inhibition; mAIH: moderate acute intermittent hypoxia. Drug doses: morphine, 4mg/Kg; TLR4 inhibitor, 10 mg/Kg.

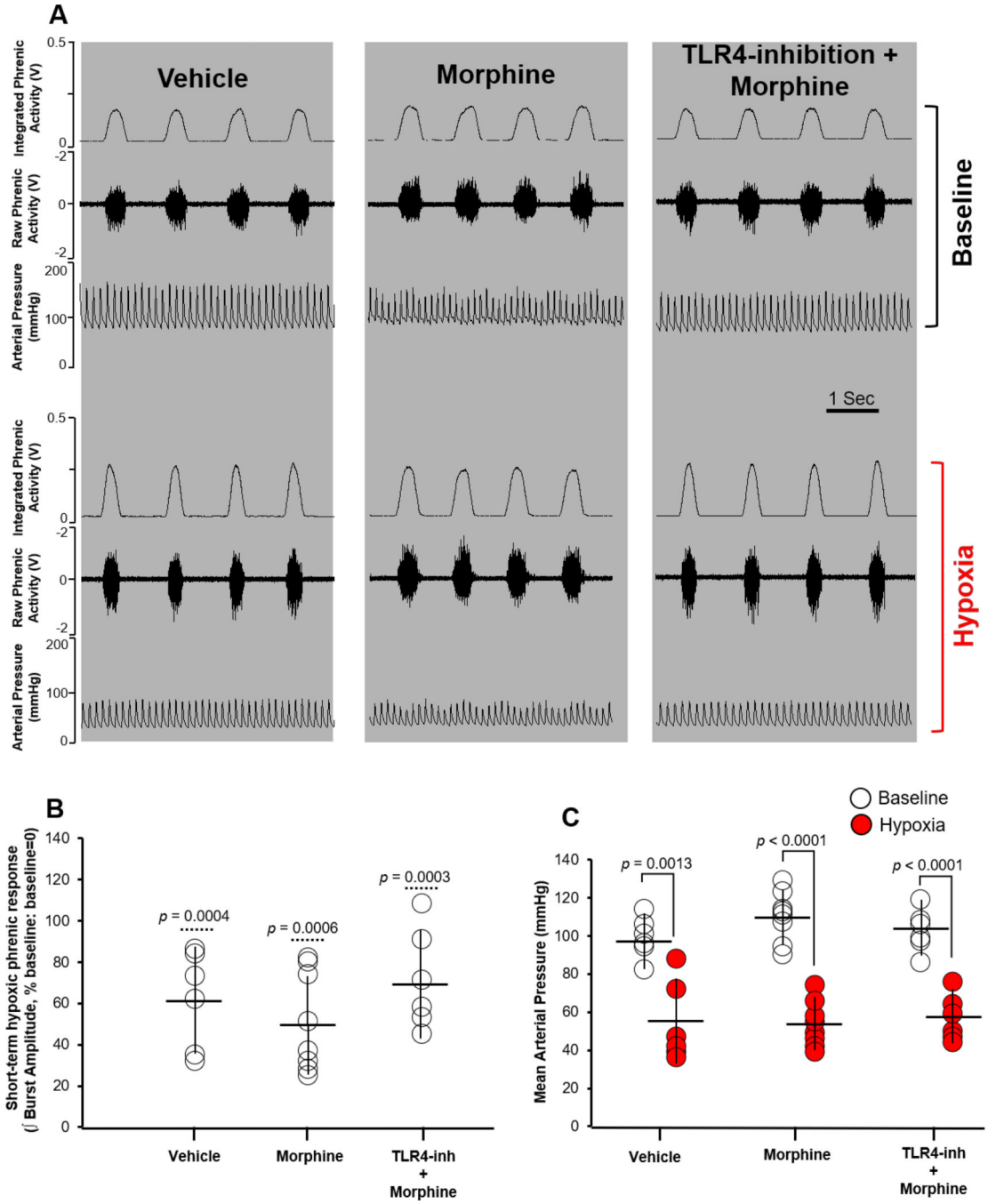

Figure 2. Short-term phrenic response and mean arterial blood pressure during hypoxia in different treatment groups.

A, Representative phrenic nerve neurogram traces demonstrate raw (middle traces) and integrated (top traces) phrenic nerve activity during baseline, and during the last minute of a 5-min hypoxic challenge. Bottom traces in each panel represent arterial pressure during baseline and during hypoxia. **B**, Normalized, inspiratory phrenic nerve burst amplitudes were similarly enhanced within hypoxic episodes in groups exposed to mAIH— phrenic amplitude was significantly increased during hypoxia as compared to baseline levels

within each group, but there was no difference comparing the hypoxic responses. **C**, Mean arterial blood pressures (mmHg) during baseline conditions and hypoxic episodes (red); no between-group differences were observed; hypoxia significantly decreased mean arterial pressure in all groups to the same degree. Solid horizontal line within each data series indicates average group mean, and the vertical bar protruding above and below the horizontal line indicates standard deviation for each data set. Each circle indicates an individual data point from a rat subject within each experimental group. Within group comparisons were made using a paired t-test (p value indicated above dashed horizontal line, panel B). Between group comparisons were made using a one-way ANOVA followed by a Tukey post-hoc test. TLR4-inh: TLR4 inhibition; mAIH: moderate acute intermittent hypoxia. Drug doses: morphine, 4mg/Kg; TLR4 inhibitor, 10 mg/Kg.

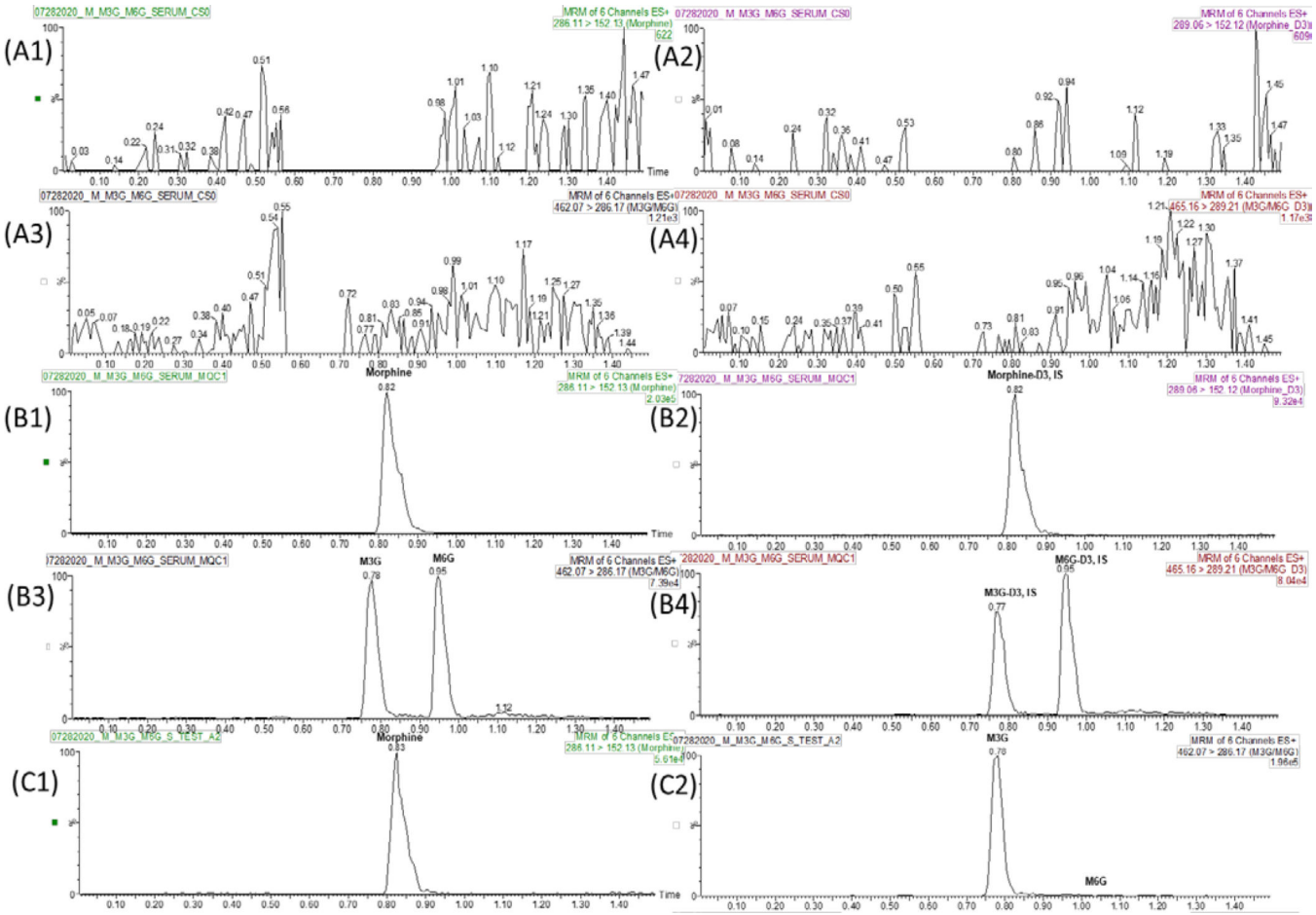

Figure 3. Representative multiple-reaction monitoring chromatograms.

(A1) morphine, (A2) morphine-D3 (IS), (A3) morphine 3-glucuronide (M3G) and morphine-6-glucuronide (M6G), (A4) M3G-D3 and M6G-D3 (IS) in drug-free rat serum, (B1) morphine (90 ng/ml), (B2) morphine-D3 (IS, 10 ng/ml), (B3) M3G and M6G (90 ng/ml, each), (B4) M3G-D3 and M6G-D3 (IS, 10 ng/ml each) spiked in drug-free rat serum, (C1) morphine, and (C2) M3G and M6G in serum samples 4.5 hr after subcutaneous morphine (4 mg/kg) administration.

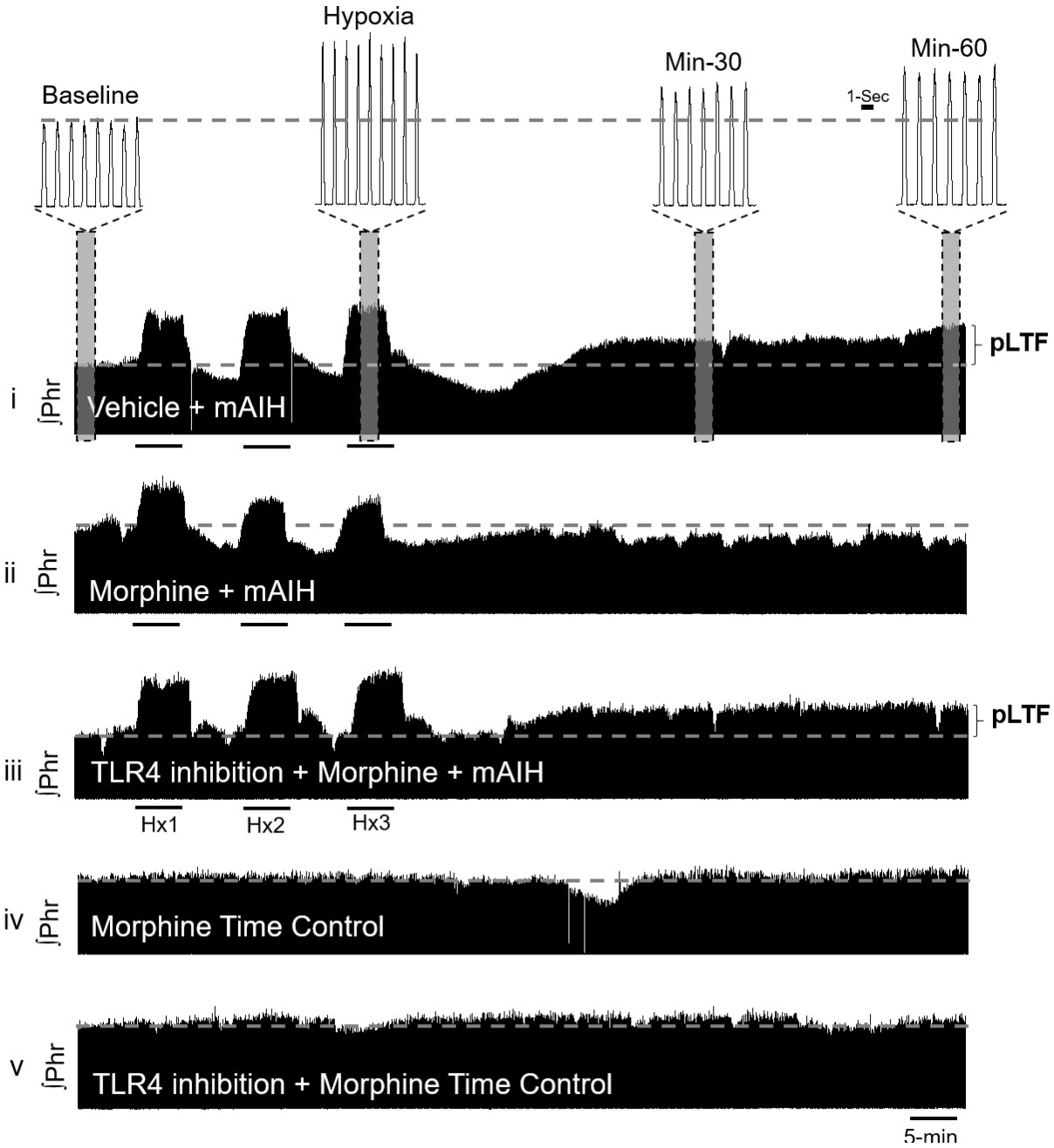

Figure 4. Representative phrenic recordings showing systemic morphine blocks phrenic long-term facilitation via TLR4 signaling.

Representative integrated inspiratory phrenic (Phr) nerve traces before, during and 60-minutes after moderate acute intermittent hypoxia (mAIH) in rats pre-treated 3 hours prior with systemic vehicle (i), morphine (4mg/Kg) (ii), or combination of TLR4 inhibition, (+)-naloxone (10mg/Kg), and morphine (iii). Second to last trace (iv) represents a phrenic neurogram recording from a time-matched morphine-treated control rat. Bottom trace (v) represents a trace recording from a time-matched control rat pre-treated with the TLR4 inhibitor and morphine. Note presence of phrenic long-term facilitation (pLTF) in a vehicle treated rat (i) showing example inspiratory phrenic nerve bursts in short time scale on

top, absence with morphine treatment (ii), and restoration with TLR4 inhibition prior to morphine delivery (iii). Hx: hypoxic exposure 1, 2 and 3.

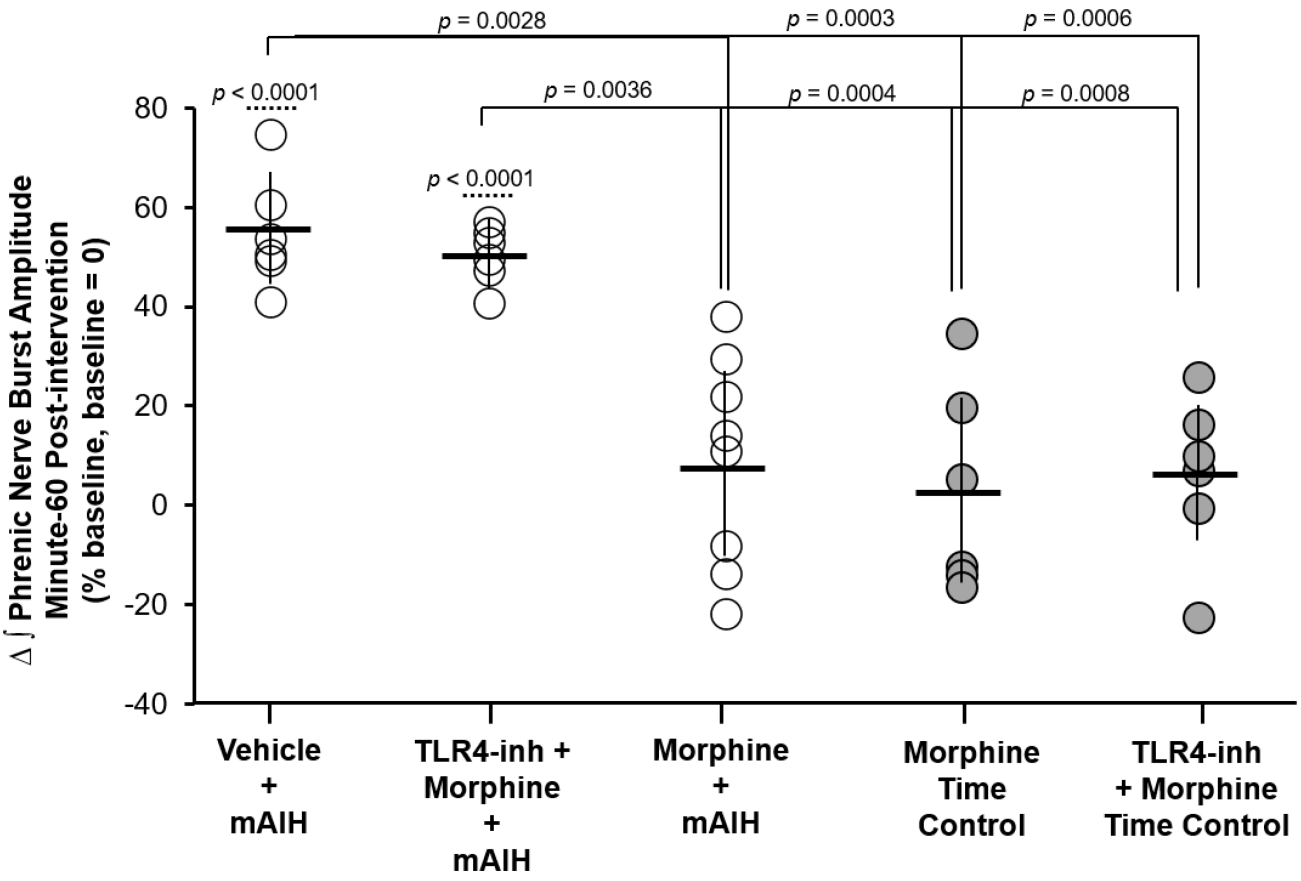

Figure 5. Morphine blocks phrenic long-term facilitation via mechanisms that require TLR4 activation.

Group data expressed as percentage change from baseline, showing that moderate acute intermittent hypoxia (mAIH) triggers pLTF in vehicle treated rats; at 60-min post hypoxia, phrenic nerve activity was significantly elevated above baseline ($p < 0.0001$). In rats pre-treated with morphine (4mg/Kg), pLTF was absent. Pre-treatment with the TLR4 inhibitor, (+)-naloxone (10mg/Kg), prevented morphine-induced impairment of pLTF: like vehicle treated rats, phrenic nerve amplitude was significantly increased above baseline levels at 60-min post hypoxia ($p < 0.0001$). Phrenic nerve activity remained near baseline levels across the 60-min recording period in time-matched drug-treated rats that did not get exposed to mAIH (i.e., time controls). Solid horizontal line within each data series indicates average group mean, and the vertical bar protruding above and below the horizontal line indicates standard deviation for each data set. Each circle indicates an individual data point from a rat subject within each experimental group. Between group comparisons were made using a one-way ANOVA, followed by a Tukey significance post hoc test. TLR4-inh: TLR4 inhibition.

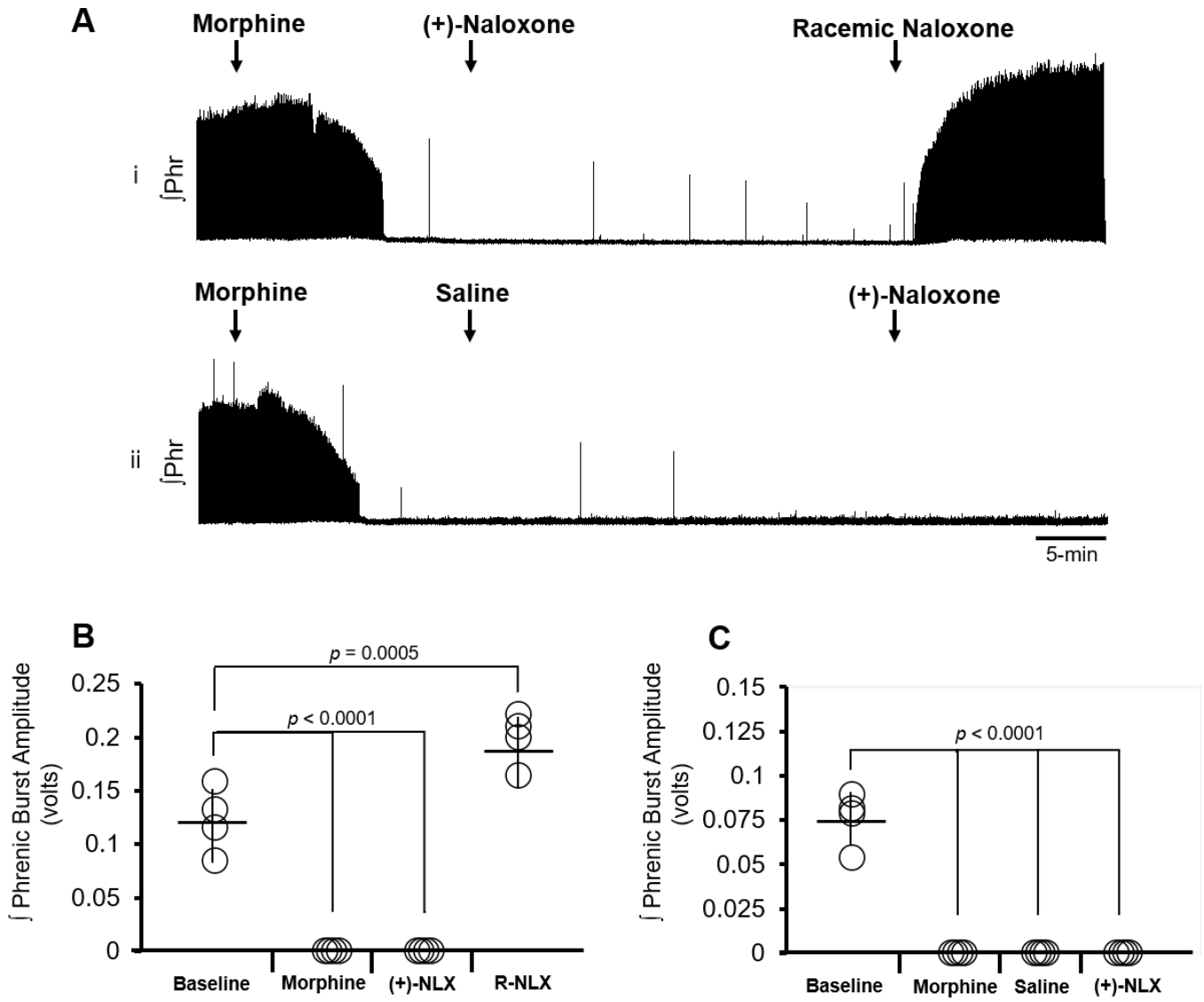

Figure 6. (+)- Naloxone does not interfere with respiratory depressive effects of morphine operating at mu opioid receptors.

A, Representative integrated inspiratory phrenic (Phr) nerve traces demonstrating the action of acute morphine injection (4mg/Kg) on phrenic motor output during terminal neurophysiological recordings. Ai, Subcutaneous morphine injection potently depresses respiratory motor output. Respiratory activity remains absent following (+)-naloxone (10mg/Kg) delivery. Racemic naloxone (mixture of mu opioid receptor antagonist + TLR4 inhibitor) administration (1mg/Kg) quickly reverses morphine-induced respiratory depression. Aii, Time control recording demonstrating that (+)-naloxone does not reverse respiratory depression induced by systemic morphine. **B** and **C**, Group data demonstrating that delivery of morphine consistently abolishes phrenic motor output. Respiratory depression can only be reversed with racemic naloxone (B), but not with the TLR-4 antagonist, (+)-naloxone (C), demonstrating that the (+)- stereoisomer of naloxone does not antagonize mu opioid receptors. B and C are two separate experimental rat groups, reflecting raw trace examples illustrated in Ai and Aii, respectively. Each circle indicates an individual

data point from a rat subject within each experimental group. Between group comparisons were made using a one-way ANOVA, followed by a Tukey significance post hoc test. NLX: naloxone. R-NLX: Racemic naloxone.

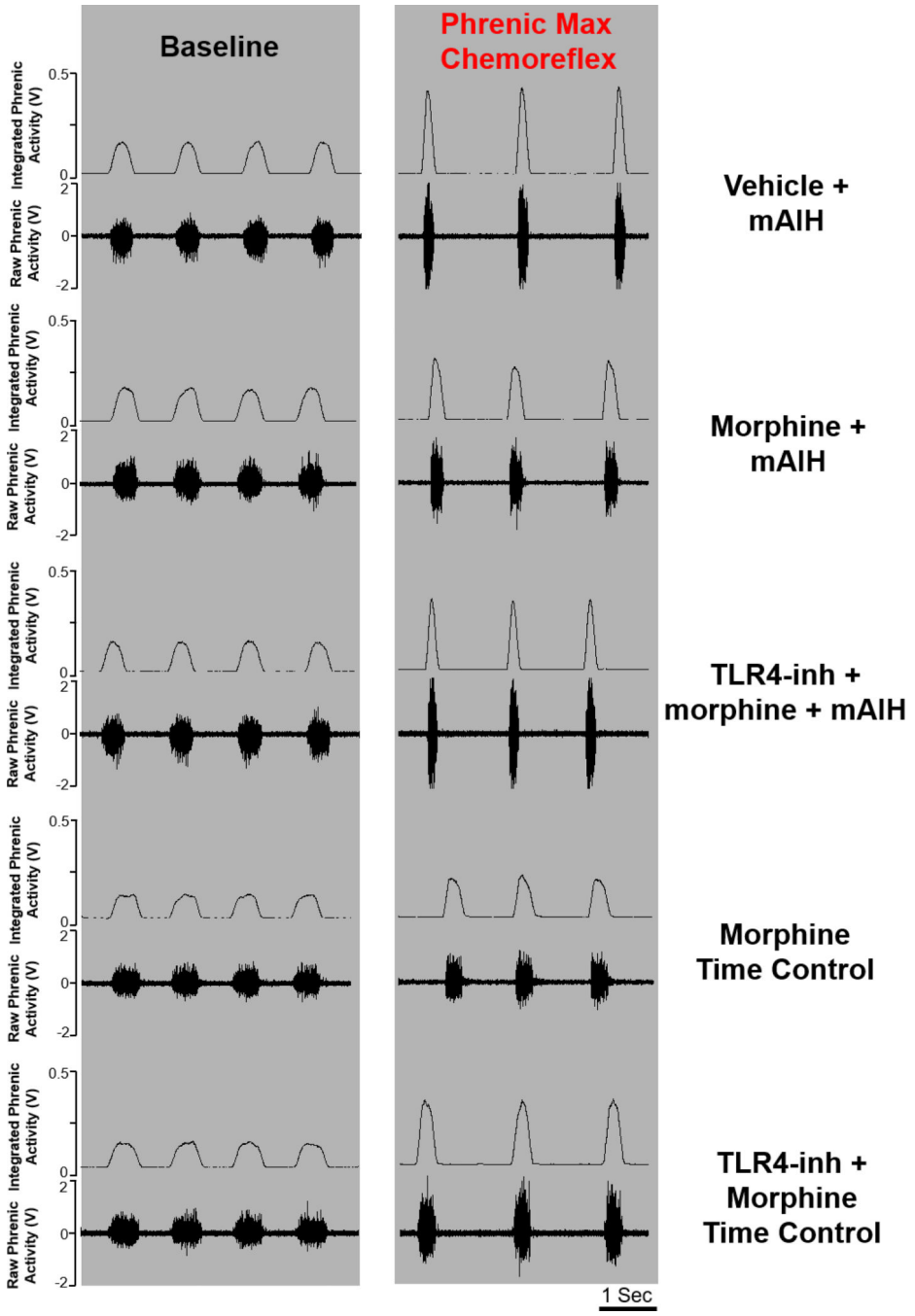

Figure 7. Phrenic nerve activity during baseline and max chemoreflex stimulation in all groups.

Representative phrenic nerve neurogram traces demonstrate raw (bottom) and integrated (top) phrenic nerve activity during baseline, and during the last minute of a 2-min hypoxic hypercapnic challenge in various treatment groups. Max chemoreflex responses to hypoxic hypercapnia (10% O2, 7% CO2 and balance N2) were recorded at the end of each neurophysiological recording period: either at 60-minutes post moderate acute intermittent hypoxia, or at an equivalent time point in time control studies.

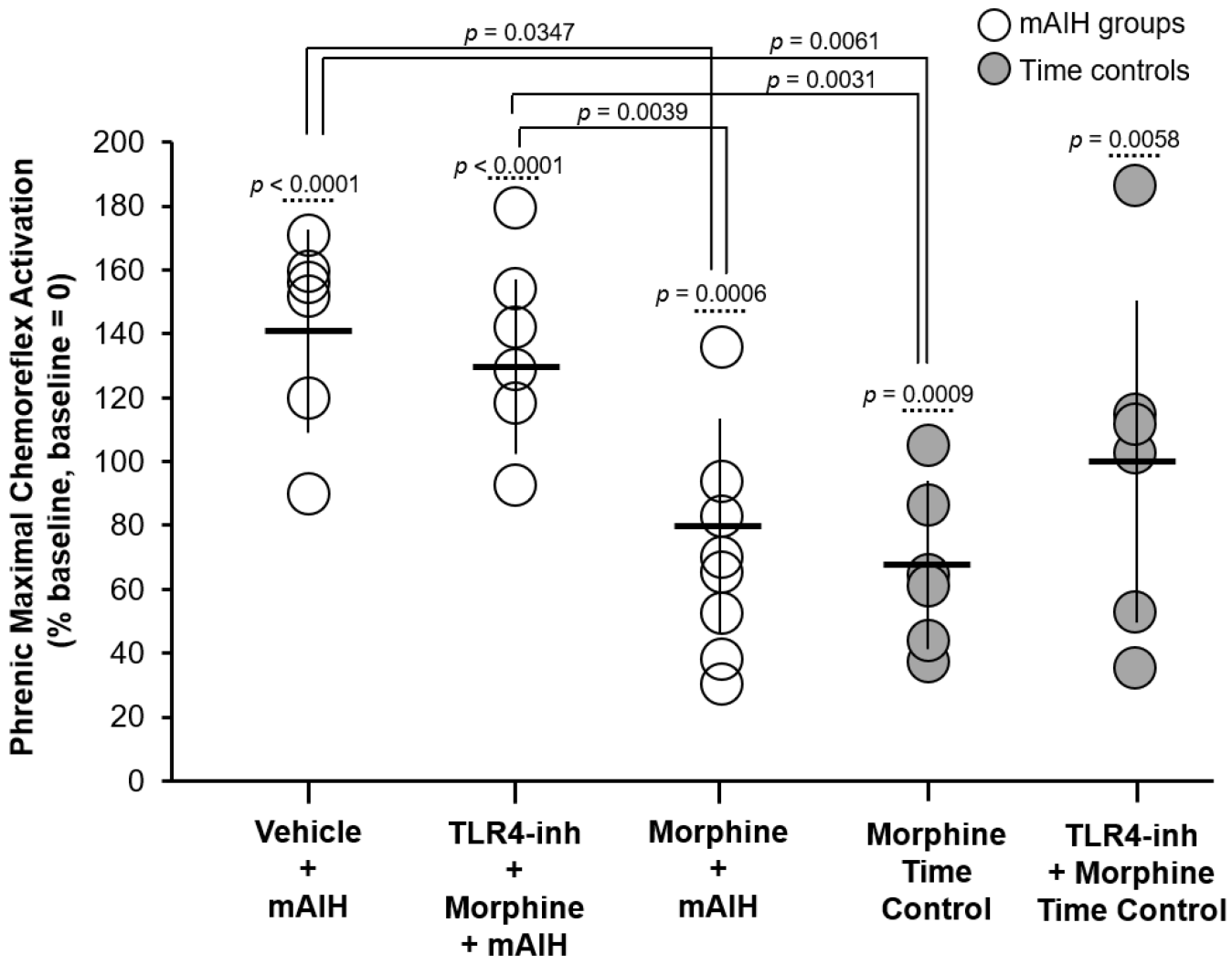

Figure 8. Morphine depresses phrenic response to maximal chemoreflex activation.

Group data showing enhancement in phrenic burst amplitude in response to hypoxic hypercapnia in various treatment groups. Although maximal chemoreflex activation significantly increased phrenic burst amplitude within each treatment group as compared to baseline values ($p < 0.05$ within each group), the relative increase was significantly reduced in morphine + mAIH, or morphine time controls versus vehicle or the group receiving combined TLR4 inhibition + morphine + mAIH. All groups were exposed to hypoxic hypercapnia at the end of each neurophysiology recording. Solid horizontal line within each data series indicates average group mean, and the vertical bar protruding above and below the horizontal line indicates standard deviation in each data set. Circles indicate individual data points from each rat subject within the experimental groups. Open circles are maximal chemoreflex responses recorded from rats at 60-minutes after exposures to moderate acute intermittent hypoxia (mAIH). Grey circles are individual responses at the end of each time control recording. Within group comparison versus baseline values was made using a paired t-test. Between group comparisons were made suing a one-way ANOVA, followed

by a Tukey significance post hoc test. TLR4-inh: TLR4 inhibition. Drug doses: morphine, 4mg/Kg; TLR4 inhibitor, 10 mg/Kg.

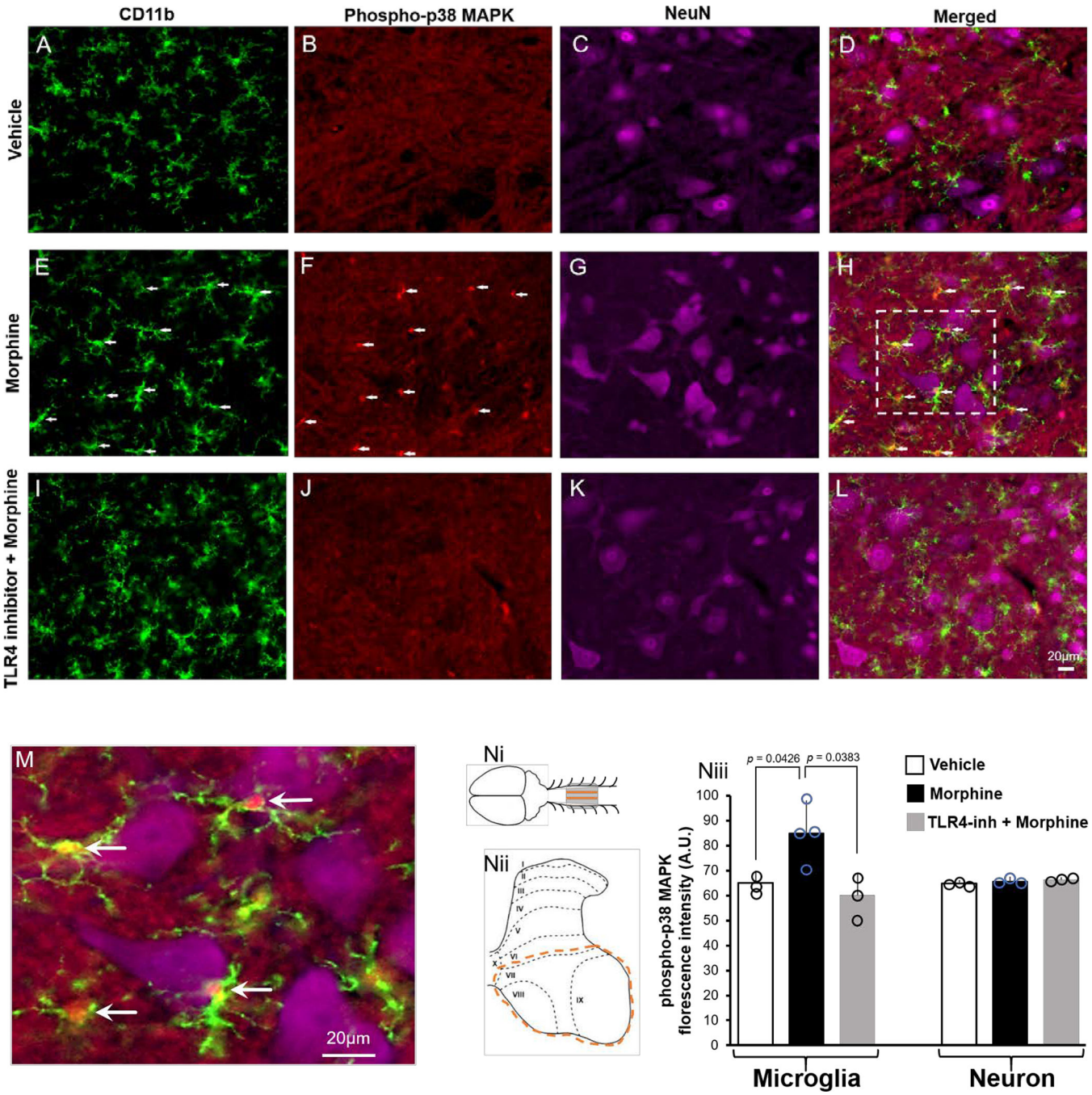

Figure 9. Morphine increases cervical spinal microglial p38 MAPK phosphorylation via a TLR4-dependent mechanism.

A-L, Triple immunofluorescent staining illustrating cervical spinal CD11b (green, microglial marker), phosphorylated p38-MAPK (red, examples marked by arrows) and NeuN (purple, neuronal marker) localization approximately 4.5 hours following systemic delivery of either vehicle (a-d), morphine (e-h) or TLR-4 inhibitor with morphine (i-l). Representative images are from the ventral horn of the cervical (~C4) spinal cord. Presumptive phrenic motor neurons are large, NeuN- positive cells in the anatomical region

pertaining to the phrenic motor nucleus. Images demonstrate heavy phospho-p38 MAPK and CD11b co-localization in morphine-treated animals (white arrows). There was no co-localization of phospho-p38 MAPK and NeuN in any experimental group. **M**, Higher magnification of CD11b and NeuN immunoreactive cells from the square marked in panel H, demonstrating phospho-p38 MAPK (red) co-localization (white arrows) within microglia (green), but not neurons (purple) in a morphine-treated animal. **Ni and Nii**, Phospho-p38 MAPK fluorescence intensity was assessed in C3-C5 (grey square, Ni) segment of the ventral cervical spinal horns, encompassing laminae VII, VIII and IX (dashed orange line, Nii). **Niii**, Average group data demonstrating that systemic morphine significantly enhances phosphorylated p38-MAPK levels within CD11b-positive cells as measured by optical fluorescence density analysis. Pretreatment with the TLR4 inhibitor, (+)-naloxone, prevented morphine-mediated phospho-p38 MAPK upregulation in CD11b-positive cells, demonstrating that morphine-induced p38 MAPK phosphorylation/activation requires TLR4 signaling. None of the drug treatments alter phosphorylated p38-MAPK levels within NeuN-positive cells. Data are means + standard deviation. Circles indicate average fluorescence intensity of all images from each animal subject within each respective treatment group. Between group comparisons were made using a one-way ANOVA, followed by a Tukey significance post hoc test. TLR4-inh: TLR4 inhibition; A.U.: arbitrary units. Drug doses: morphine, 4mg/Kg; TLR4 inhibitor, 10 mg/Kg.

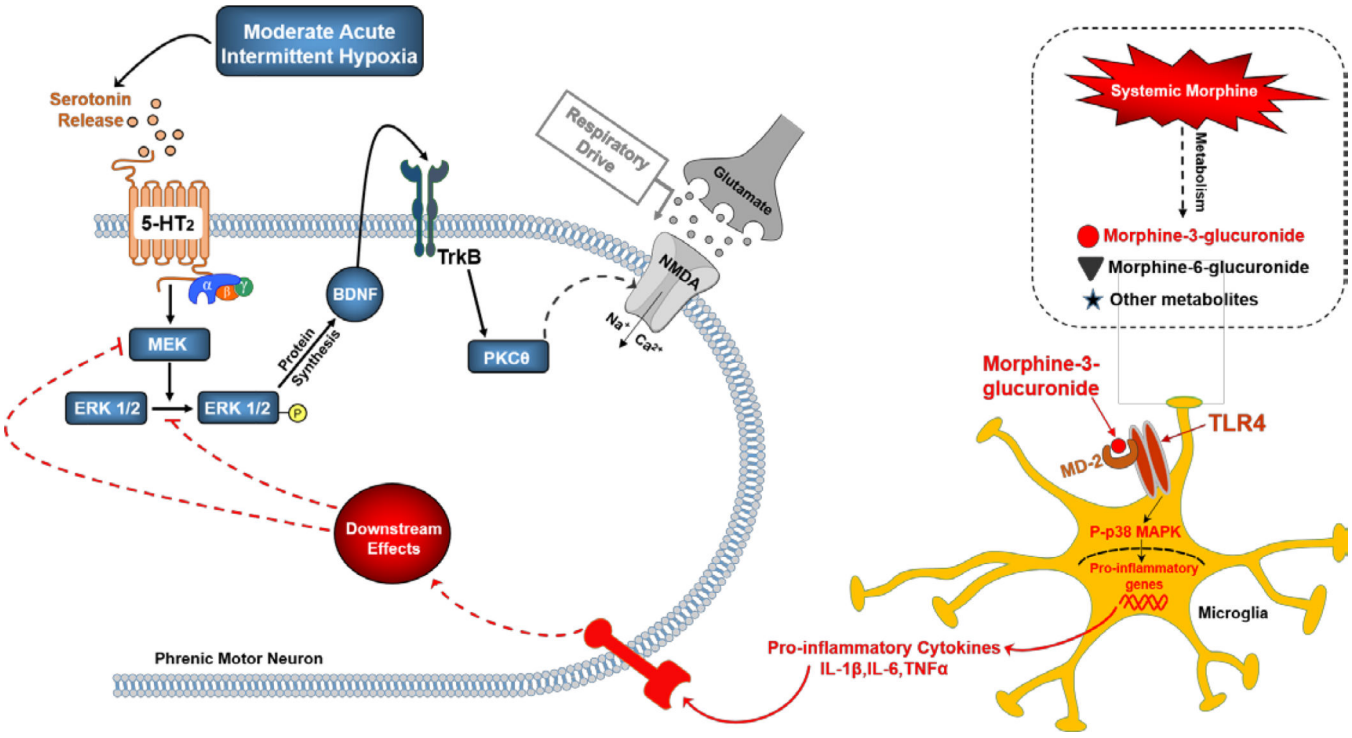

Figure 10. Proposed mechanism of morphine-induced inhibition of moderate acute intermittent hypoxia-induced phrenic long-term facilitation (pLTF).

Moderate acute intermittent hypoxia (mAIH) triggers serotonin (5-HT) release on/near phrenic motor neurons. Activation of phrenic 5-HT type 2 receptors initiates downstream signaling, leading to phosphorylation of ERK 1/2 MAPK and subsequent BDNF protein synthesis. Activation of TrKB signaling by BDNF propagates the cascade to enhance synaptic efficacy and increase in excitatory respiratory drive onto phrenic motor neurons. This enhanced excitatory drive manifests itself as long-lasting enhancement of phrenic motor output (i.e., pLTF). In the proposed model, morphine is metabolized into morphine-3-glucuronide (M3G), morphine-6-glucuronide (M6G) and other metabolites. M3G binds to the microglial TLR4-MD-2 complex, initiating an innate immune response that involves p38 MAPK phosphorylation/activation and downstream pro-inflammatory gene expression/cytokine production. Pro-inflammatory cytokines consequently activate downstream signaling within the phrenic motor pool that inhibit mAIH-induced plasticity of phrenic motor neuronal synapses (e.g. pLTF). Pro-inflammatory cascades may inhibit pLTF by acting at multiple sites: they may negatively regulate 5-HT2 signaling at the level of MEK and/or at the ERK 1/2 activation loop. Inhibition of TLR4 signaling prior to morphine delivery permits 5-HT2-mediated MEK-ERK1/2 signaling, leaving mAIH-induced pLTF unperturbed. Broken lines: undefined inhibitory feedback site at or below MEK level. Broken arrows: hypothesized pathway with unknown precise mechanism in the proposed model. TLR4-MD2 complex: Toll-like receptor 4 (TLR4)–myeloid differentiation factor 2 (MD2) complex; P-p38 MAPK: phosphorylated p38 MAPK. Adapted and modified from Tadjalli et al., 2021.

Table 1.

Mass spectrometer compound parameters for morphine, morphine-3-glucuronide, morphine-6-glucuronide and internal standards (IS)

Compound	Mass transition (*m/z*)	Cone Voltage (V)	Collision Energy (V)
Morphine	286.11 > 152.13	34	62
Morphine-D3 (IS)	289.06 > 152.12	56	60
Morphine-3-glucuronide	462.07 > 286.17	42	30
Morphine-3-glucuronide-D3 (IS)	465.16 > 289.21	48	32
Morphine-6-glucuronide	462.07 > 286.17	42	30
Morphine-6-glucuronide-D3 (IS)	465.16 > 289.21	48	32

Table 2.

Physiological variables measured during electrophysiological experiments

Experimental Groups	$PaCO_2$ (mmHg)	PaO_2 (mmHg)	SBEc mmol/L	pH
Vehicle + mAIH				
Baseline	41.5 ± 3.1	262 ± 22	1.9 ± 1.9	7.41 ± 0.02
Hypoxia	39.9 ± 2.0	39.5 ± 6	−0.13 ± 1.7	7.39 ± 0.02
30 min	41.3 ± 2.6	221 ± 26	0.53 ± 1.4	7.40 ± 0.03
60 min	42.9 ± 3.5	251 ± 15	2.0 ± 2.3	7.40 ± 0.03
Morphine + mAIH				
Baseline	38.7 ± 2.7	282 ± 36	2.2 ± 1.6	7.44 ± 0.04
Hypoxia	38.9 ± 2.3	39.9 ± 4	1.5 ± 2.1	7.42 ± 0.04
30 min	39.4 ± 2.2	237 ± 42	0.1 ± 1.2	7.40 ± 0.03
60 min	39.9 ± 3.5	247 ± 38	0.3 ± 1.4	7.41 ± 0.03
TLR4 inhibition + Morphine + mAIH				
Baseline	42.7 ± 3.0	293 ± 21	2.3 ± 1.6	7.41 ± 0.04
Hypoxia	42.6 ± 2.6	43.1 ± 5	2.2 ± 1.17	7.42 ± 0.03
30 min	43.0 ± 2.5	247 ± 29	0.85 ± 1.6	7.39 ± 0.01
60 min	43.7 ± 2.8	264 ± 13	0.48 ± 2.1	7.38 ± 0.02
Morphine Time Control				
Baseline	40.4 ± 5.0	260 ± 24	2.0 ± 1.4	7.43 ± 0.01
30 min	39.5 ± 6.2	254 ± 26	−0.2 ± 1.3	7.41 ± 0.02
60 min	39.9 ± 4.7	267 ± 24	0.4 ± 3.1	7.41 ± 0.02
TLR4 inhibition + Morphine Time Control				
Baseline	44.0 ± 2.0	299 ± 31	2.9 ± 1.4	7.41 ± 0.02
30 min	44.2 ± 1.6	264 ± 36	0.3 ± 2.0	7.37 ± 0.03
60 min	43.7 ± 3.4	258 ± 31	0.9 ± 2.0	7.38 ± 0.04

Values are means ± standard deviation. $PaCO_2$, arterial carbon dioxide pressure; PaO_2, arterial oxygen pressure; SBEc, blood standard excess base; mAIH, moderate acute intermittent hypoxia. Time controls represent equivalent time-matched measurements in rat subjects that did not receive mAIH during neurophysiological recordings.

Table 3.

Serum concentrations of morphine, morphine-3-glucuronide, and morphine-6-glucuronide

	Concentration (ng/ml)		
Subject	**Morphine**	**Morphine-3-glucuronide**	**Morphine-6-glucuronide**
R1	18.7	222.5	-
R2	24.4	139.5	-
R3	12.9	215.5	-
R4	17	481	-
R5	10.1	449	-
R6	9.6	434.5	-
Average	**15.5 ± 6**	**323.7 ± 147**	

Values are means ± standard deviation. Whole blood was collected 4.5 hours following a single morphine injection (subcutaneous, 4mg/kg). Isolated blood serum was then analyzed for morphine, morphine-3-glucuronide and morphine-6-glucuronide content. Morphine-6-glucuronide was below the lower limit of quantification (<1 ng/ml).